land

MDPI

Article

Multi-Dimensional Collaborative Optimization and Performance Assessment of Barrier Removal, Structural Robustness, and Carbon Sink Enhancement in the Beijing-Tianjin-Hebei Ecological Network

Yuanyuan Pei [1], Zhi Zhou [1,2,3,*], Xing Gao [4] and Pengtao Zhang [1,2,3]

[1] College of Land and Resources, Hebei Agricultural University, Baoding 071001, China; peiyuanyuan1104@163.com (Y.P.); zhangpt@hebau.edu.cn (P.Z.)
[2] Field Scientific Observation and Research Station of Land Resource Utilizaton Around Bohai Sea, Ministry of Natural Resources, Cangzhou 061014, China
[3] Rural Culture and Rural Governance Research Center, Hebei Agricultural University, Baoding 071001, China
[4] School of Public Administration, Hebei University of Economics and Business, Shijiazhuang 050062, China; gaoxing@hueb.edu.cn
* Correspondence: zhouzhi797825@163.com

Abstract

Ecological network optimization can enhance ecological connectivity, regional ecological stability, and carbon sink capacity. Current research on ecological networks employs single-perspective optimization, which overlooks the synergistic requirements between network topological characteristics and the dual carbon goals. It lacks a comprehensive, systemic optimization framework. Focusing on the Beijing–Tianjin–Hebei region, the work constructs an ecological network by integrating ecosystem services, morphological spatial pattern analysis (MSPA), and circuit theory. A framework integrating barrier removal, structural robustness, and carbon sink enhancement is proposed, incorporating ecological barrier identification, complex network theory, and carbon offset patterns for multi-objective structural and functional optimization. The optimized network is evaluated using structural metrics, robustness analysis, and carbon sequestration validation. The network comprises 41 ecological sources and 102 corridors, exhibiting a dense northwest and sparse southeast distribution. Ecological barriers totaling 565.56 km^2 are removed to improve connectivity in the region. An edge-addition strategy introduces 12 nodes and 49 edges, enhancing connectivity, stability, and carbon sink capacity. Restoration priorities are set with the phased objectives of removing barriers, connecting topological weak points, and optimizing low-value carbon offset areas. Shifting the focus from structural connectivity to integrated function, the work contributes a methodological framework for advancing ecological security and carbon neutrality in urban agglomerations.

Keywords: ecological network enhancement; ecological network identification; complex network; carbon offset; circuit theory; Beijing-Tianjin-Hebei (BTH) region

Check for updates

Academic Editor: Shiliang Liu

Received: 6 January 2026
Revised: 9 February 2026
Accepted: 24 February 2026
Published: 26 February 2026

Copyright: © 2026 by the authors. Licensee MDPI, Basel, Switzerland. This article is an open access article distributed under the terms and conditions of the Creative Commons Attribution (CC BY) license.

1. Introduction

China's rapid urbanization and agricultural scaling have significantly altered land use patterns and landscape structures [1], triggering ecological security issues (e.g., the shrinkage of natural spaces, habitat destruction, and landscape fragmentation) [2]. As the

primary source of carbon emissions from human activities, cities contribute to approximately 75% of global carbon emissions [3], with the proportion exceeding 85% in China [4]. Intensive industrial activities and dense spatial configurations exacerbate the imbalance in carbon sinks and carbon sources [5]. Against the backdrop of the national Dual Carbon Goals, safeguarding ecological security and balancing carbon budgets have emerged as dual imperatives demanding coordinated advancement. As the economic core of northern China and a critical ecological zone, the Beijing-Tianjin-Hebei (BTH) region is affected by vegetation degradation in mountainous areas, habitat fragmentation in plains, and the concentration of high-energy-consumption industries. The region's development is constrained by three critical constraints: limited ecological carrying capacity, fragmented ecological connectivity, and a significant spatial imbalance between carbon emission sources and sequestration sinks. Ecological networks can optimize landscape configuration, ecological connectivity and systemic stability, and biodiversity conservation [6,7]. However, existing research predominantly focuses on enhancing the structural connectivity of ecological networks, failing to integrate carbon offset requirements into the entire process of network construction and optimization. This limitation undermines the integrated management of ecological and climate security, a core requirement for achieving the dual carbon goals.

Current practices in ecological network construction typically follow the workflow of determining source areas, creating resistance surfaces, and extracting corridors [8]. Ecological source identification primarily employs single methods such as MSPA [9], ecosystem service functions [10], and landscape connectivity analysis [11]. Therefore, a systematic source identification method is adopted, integrating structural and functional criteria [12]. The study overcomes the lack of comprehensiveness and relational depth inherent in conventional single-dimensional approaches to source identification. Ecological resistance surfaces' construction is mostly supported by the assignments of comprehensive factors, e.g., natural conditions and human disturbances [13,14]. Ecological corridors are extracted by determining the least-cost path based on the minimum cumulative resistance (MCR) model [15] and by identifying critical nodes using circuit theory [16]. This framework enables ecological network analysis from the connections between corridors and source areas. Contemporary research into ecological network optimization is predominantly centered on bolstering landscape connectivity [17]. Such optimization is realized by establishing ecological corridors, stepping stones, or additional ecological sources [18]. As theoretical research advances, studies on ecological network optimization are increasingly characterized by interdisciplinary integration and technological convergence. This evolution is marked by a growing emphasis on enhancing ecosystem services and promoting regional sustainable development [19–21]. In terms of evaluating ecological network optimization outcomes, initial research primarily focuses on network connectivity indices, with an emphasis on assessing structural connectivity [22,23]. Following the introduction of complex network theory, robustness assessment has become a research focus [24]. This approach evaluates the structural stability and disturbance resistance of a network by simulating random node removals or targeted attacks [25]. Critical nodes and vulnerable components within the network are identified by analyzing connectivity changes from the removal of ecological sources or corridors.

Current research still faces two major limitations. Firstly, the identification methods for ecological sources remain simplistic, struggling to systematically integrate structural and functional correlations. Traditional approaches to ecological network construction prioritize methodologies such as MSPA [26] or the MCR model [27] to identify ecological sources, corridors, and nodes [28]. However, these methods overly rely on landscape patch characteristics for source identification [29] and neglect ecosystem service functions [30]. Consequently, they fail to reflect the intricate relationship between the structural connectiv-

ity and functional connectivity of ecosystems. Secondly, the application of complex network theory has largely been confined to analyzing local indices, with limited exploration of the internal mechanisms of the network from a holistic topological perspective. Complex network theory reveals the interconnections between elements within a network [31,32]. Few studies comprehensively integrate multiple topological characteristics to analyze the complex relationships within the internal structure of ecological networks [33]. Thirdly, A critical gap exists in urban carbon emissions and sequestration. Urban construction generates high carbon emissions. Its expansion further weakens regional carbon sequestration, exacerbating carbon budget imbalance [34]. Some studies have attempted to incorporate carbon emissions as a resistance factor or include carbon sinks in the source identification system [35]. A systematic research framework, fully embedding carbon offset mechanisms into the entire process of network optimization and effectiveness evaluation, has not yet been established [36]. Additionally, current research still exhibits insufficient assessment of ecosystem service functions before and after optimization, particularly regarding carbon sequestration capacity [37].

Ecological network optimization serves as a critical strategy to address ecological challenges. It aims to maintain regional ecological security and promote sustainable development by enhancing connectivity, robustness, and ecosystem service functions [9]. Removing barriers significantly enhances ecological network connectivity, which reinforces structural robustness. Thus, ecosystems can perform carbon sequestration [38]. Networks with high robustness are better equipped to withstand disturbances, ensuring the long-term stability of carbon sink functions [39]. As a key regulating ecosystem service, carbon sequestration exhibits a significant coupling relationship with the structural characteristics of ecological networks [40]. The planning and management of ecological networks shall fully consider the synergistic effects of these three dimensions to maximize ecosystem services and ensure sustainable regional ecological security. The work proposes an integrated barrier removal-structural robustness-carbon sequestration enhancement assessment framework to elucidate the synergistic mechanisms between structural optimization and functional improvement.

With the BTH region as the research area, the aforementioned issues were addressed through innovations in theory, methodology, and application. (1) A systematic method was proposed to identify ecological sources synergizing structure and function. (2) Based on the characteristics of network topology, a new paradigm was proposed for 3D collaborative optimization of barrier removal, structural robustness, and carbon sink enhancement. (3) A comprehensive evaluation framework was established, integrating connectivity, robustness, and carbon sink function. Thus, a systematic expansion from structural optimization to functional synergy was achieved. A multi-objective ecological network optimization framework was established to balance structure and function. The findings provide scientific support for reconstructing regional ecological security patterns, optimizing territorial space, and synergizing the dual carbon goals.

2. Materials and Methods

2.1. Study Region Overview

The BTH region is situated in the northern part of the North China Plain (Figure 1). Geographical coordinates range from approximately 36°05′ to 42°40′ N and 113°27′ to 119°50′ E, covering approximately 216,000 km^2. Centered around Beijing and Tianjin, a cohesive urban agglomeration forms by integrating 11 prefecture-level cities in Hebei Province. This region serves as an economic core in northern China and a critical area for coordinated ecological and developmental balance.

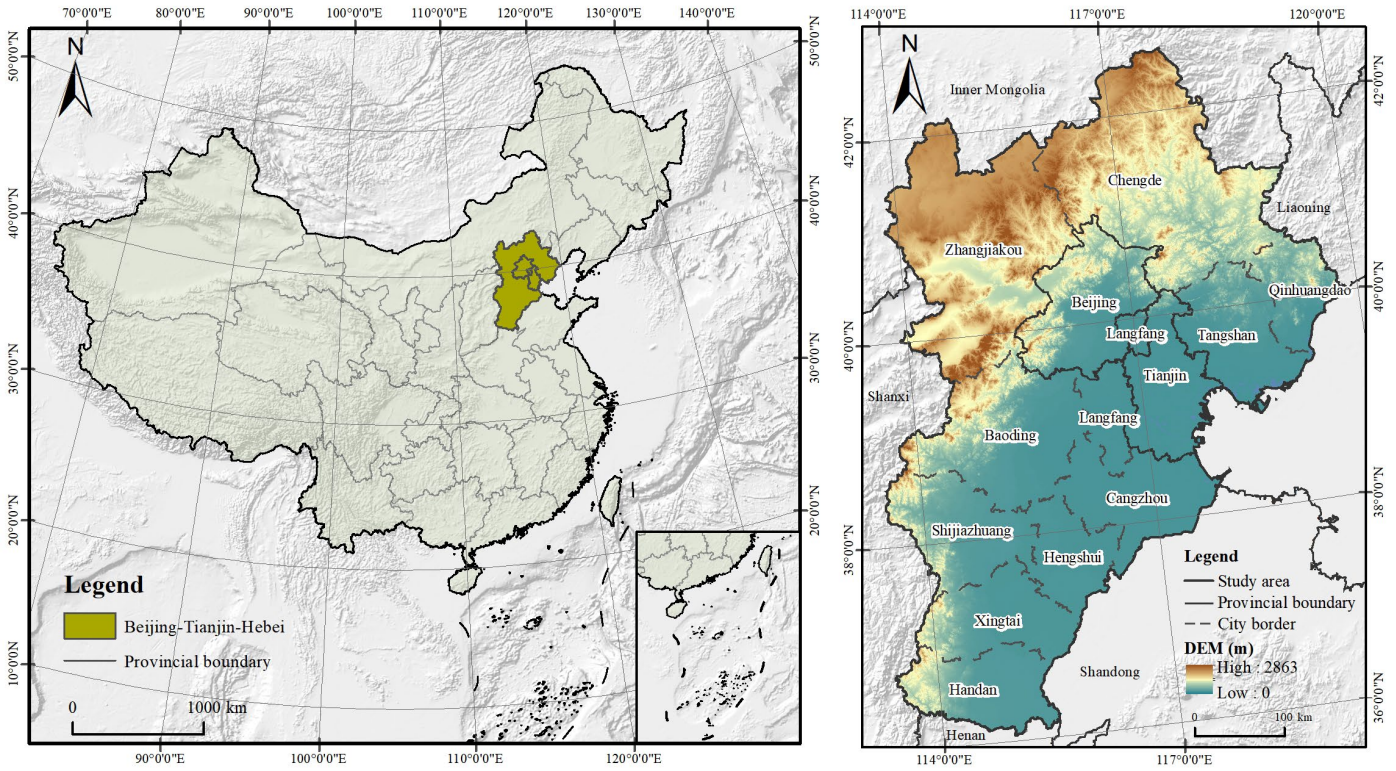

Figure 1. Location of BTH.

From a physiogeographic perspective, land slopes downward from the northwest to the southeast. The northwestern part, supported by the Yanshan and Taihang mountain ranges, consists of hilly and mountainous areas constituting over 60%. This zone functions as a core area for water conservation and biodiversity preservation. The southeastern section, comprising the North China Plain, covers about 37% of the region and serves as the main area for population, industry, and agricultural activities. Four coastal cities—Qinhuangdao, Tangshan, Tianjin, and Cangzhou—in the east boast a 640 km coastline, providing favorable conditions for land–sea coordination.

Accelerated urbanization, expansion of construction land, and energy-intensive industries in the BTH region have compressed ecological space. The dual pressures of northwestern vegetation degradation and southeastern habitat fragmentation markedly increase carbon emissions from land use changes. This places considerable pressure on ecological carrying capacity. Therefore, ecological networks should be constructed to enhance the region's carbon sink capacity, the health of the regional ecological environment, and the coordinated development of socio-economic systems.

2.2. Theoretical Basis and Analytical Framework

The construction and optimization of ecological networks involve the coupling of landscape patterns, ecological processes, and ecological functions. Its theoretical framework follows a progressive logic of pattern identification, structural optimization, functional synergy, and effectiveness evaluation, aiming to enhance regional ecological security and ecosystem service capacity [41]. Landscape ecology and ecosystem service theories provide a solid theoretical foundation for identifying ecological sources [42]. In landscape ecology, connectivity is categorized into structural connectivity and functional connectivity [43]. Functional connectivity prioritizes the actual movement capacity of species, unlike structural connectivity focusing on physical adjacency [44,45]. Functional connectivity is the result of the interaction between species behavior and landscape structure, rather than an inherent attribute of the landscape [46]. Based on the patch-corridor-matrix model, land-

scape ecology reveals the spatial constraints imposed by landscape patterns on ecological processes, highlighting the importance of spatial continuity and the integrity of ecological processes [33]. Ecosystem services theory centers on quantifying ecosystem services and identifying area 2 with high ecological values. This enables the dual integration of structural connectivity and functional importance, which overcomes the traditional research limitation of prioritizing form over function [47]. Ecosystem service importance assessment is combined with hotspot analysis to identify ecological source areas [48].

The barrier removal–structural robustness–carbon sink enhancement framework constitutes a synergistic optimization system characterized by a clear, progressive logic. Barrier removal aims to restore fundamental functional connectivity for ecological flow transmission, serving as the prerequisite for building a robust network [49]. Building upon this foundation, the topological structure is optimized to enhance the network's robustness [25,50]. Ultimately, the framework elevates the overall regional carbon sequestration capacity based on carbon offset patterns for the synergistic enhancement of connectivity, stability, and carbon sink potential [51]. Circuit theory, complex network theory, and carbon cycle theory collectively support the construction and multidimensional optimization of the ecological network throughout this process. Circuit theory identifies key corridors and barrier areas by simulating the diffusion pathways of ecological flows across heterogeneous landscapes [52–55]. This method transcends the limitation of focusing on a single optimal path by considering all potential movement pathways. A lower effective resistance between two points indicates more numerous and wider parallel paths connecting them, as well as more robust connectivity. Complex network theory is grounded in the topology of nodes and edges, revealing the overall connectivity, centrality, and robustness of a network. Thus, critical nodes and weak links are identified [56]. Habitat fragmentation and declining ecosystem service levels can be addressed by applying complex network theory to ecological network optimization [46]. Carbon cycle theory, on the other hand, quantifies carbon sequestration and carbon emissions. A carbon sequestration function-oriented approach is infused into the optimized ecological networks by identifying high carbon sequestration areas to guide the layout of corridors and nodes. As a key objective in ecological network optimization, carbon sequestration is integrated for the dual carbon goals and ecological security [57].

The integration of graph theory and percolation theory with carbon cycle theory constitutes a comprehensive evaluation framework for assessing the effectiveness of ecological network optimization. Graph theory provides a mathematical foundation for analyzing structural connectivity and complexity. It quantifies network connectivity and identifies critical hub patches or bottleneck corridors by treating habitat patches as vertices and their connections as edges. Percolation theory captures the critical thresholds of network connectivity and system resilience under disturbances. Landscape connectivity collapses abruptly rather than declines gradually once habitat loss exceeds a critical threshold [58]. For instance, connectivity may disappear entirely in a 2D lattice when the proportion of habitat falls below approximately 0.59. Carbon cycle theory, on the other hand, evaluates post-optimization gains in carbon sequestration from an ecological function perspective [59]. These theories form a multi-dimensional validation pathway encompassing structural integrity, disturbance resistance, and carbon sequestration efficacy.

Based on the support of the aforementioned multiple theories, a systematic analytical framework is constructed, including source area identification, corridor extraction, network optimization, and effectiveness evaluation (Figure 2). Step 1: Use landscape ecology and ecosystem service theory to identify ecological source areas with high connectivity and high functionality. Step 2: Construct a comprehensive ecological resistance surface using

the MCR model. Identify ecological corridors by integrating circuit theory to construct the initial ecological network.

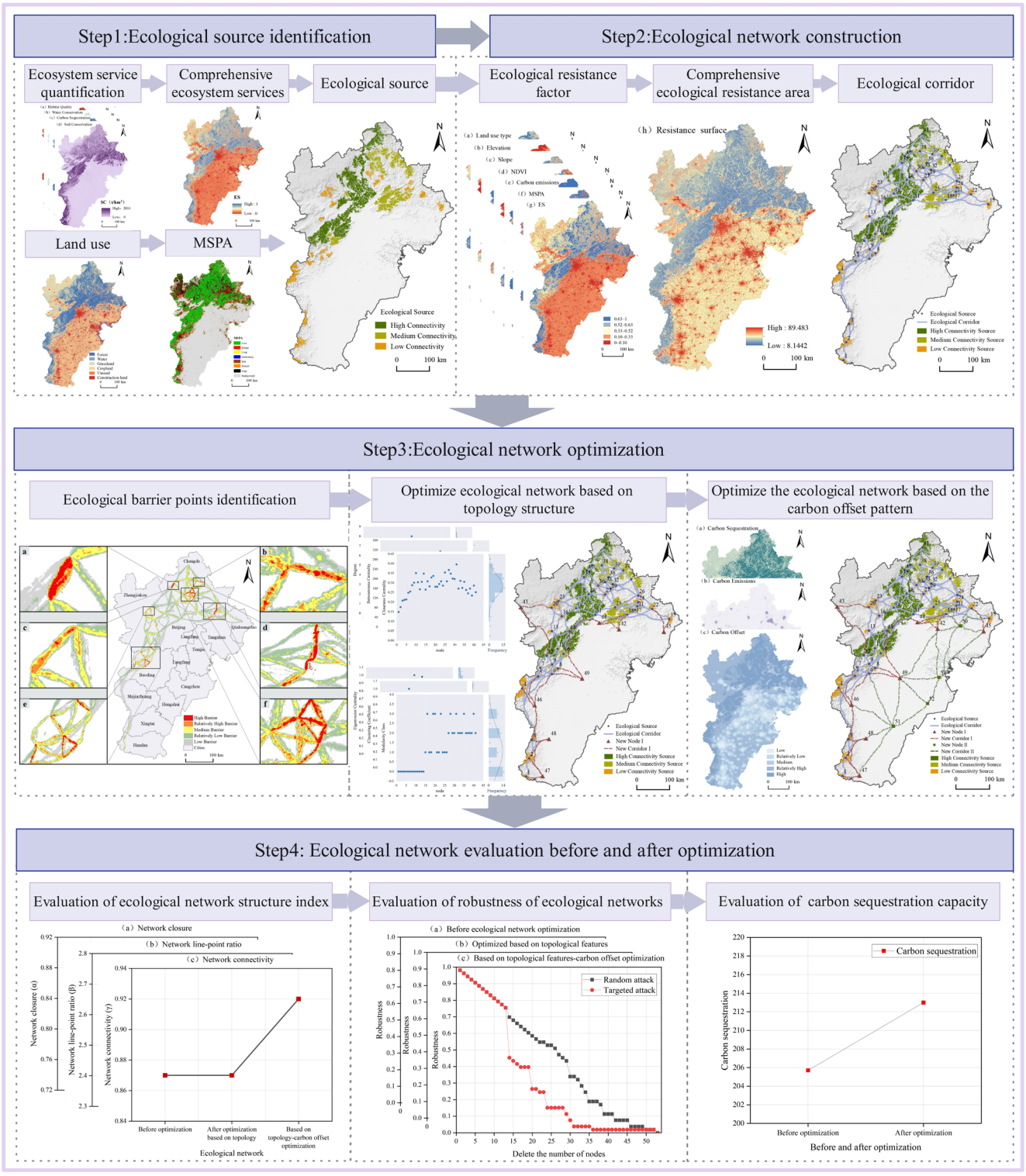

Figure 2. Theoretical framework.

Step 3: Employ the 3D collaborative optimization framework of obstacle removal, structural robustness, and carbon sink enhancement. Determine ecological barrier points based on circuit theory and optimize the topological structure by combining complex network theory. Then, introduce the carbon cycle theory to regulate the carbon sink function in low carbon offset zones. Improve ecological circulation and network robustness.

Step 4: Based on graph theory, percolation theory, and carbon cycle theory, the optimization effectiveness is validated from connectivity, structural stability, and carbon sink gains. The 3D collaborative optimization framework achieves cross-scale integration of ecological networks from static structural optimization to dynamic functional synergy. The results provide systematic support for reconstructing the ecological security pattern in the BTH region and promoting the coordinated advancement of the dual carbon goals.

2.3. Data Sources and Preprocessing

The analysis used 2023 data from the BTH region. The main datasets were as follows. (1) Data on land use for the BTH region, accessed via China Land Cover Dataset (CLCD) [60] and featured by a 30 m resolution. (2) Administrative boundary type, obtained through the National Platform for Common Geospatial Information Services. (3) Digital elevation model (DEM) data, provided by the Geospatial Data Cloud platform of the Chinese Academy of Sciences (https://www.gscloud.cn). (4) NDVI data, sourced from the National Tibetan Plateau/Third Pole Environment Data Center (https://data.tpdc.ac.cn). (5) Data on meteorological, including temperature, precipitation, and potential evapotranspiration, were obtained from the National Tibetan Plateau/Third Pole Environment Data Center (https://data.tpdc.ac.cn), with a spatial resolution of 1 km. (6) Nighttime light data, derived from the harmonized DMSP-OLS-like dataset for China [61] by integrating DMSP-OLS and NPP-VIIRS data (https://eogdata.mines.edu/products/vnl/, accessed on 23 February 2026). This dataset has undergone inter-calibration and continuity correction, with pixel digital number (DN) values of 0–63 and a spatial resolution of 1 × 1 km. (7) Energy consumption type, derived from regional official yearbooks. All datasets were uniformly projected to a unified spatial reference using GCS WGS 1984 as well as the Albers Conic Equal Area projection, with a unified spatial resolution of 1 km.

2.4. Methods for Ecological Network Identification

2.4.1. Ecological Sources' Identification

Ecological source zones are core habitats supporting the ecological network. They serve as the origins and diffusion sources of ecological flow in the source-sink theory of landscape ecology [62]. The structural perspective of landscape ecology was integrated with the functional perspective of ecosystem services to identify core patches possessing high ecological functions and good spatial connectivity. Carbon stock, habitat condition, soil conservation, and water preservation were selected as critical ecological functions in the work. All of them were spatially quantified using the InVEST model. The following approach was adopted, ensuring that the process of identifying ecological source areas was free from subjective judgment bias. All service functions considered were regarded as equally critical when each played an irreplaceable role in maintaining ecosystem health and supporting regional sustainable development. Therefore, an equal-weight overlay method was applied for a comprehensive evaluation after normalizing the assessment results of the four functions [52,63]. A composite ecosystem service map was created and classified into five levels using the natural breaks algorithm to ensure the spatial connectivity of the ultimately selected ecological source areas. Candidate areas were identified at the intersection of high-value ecosystem service zones and MSPA-derived core areas to ensure both high ecosystem function and structural connectivity in source selection [64]. This approach excluded high-value but isolated patches.

A systematic threshold sensitivity analysis was conducted to determine the minimum area threshold for source patches [65]. Thresholds ranging from 10 to 200 km^2 were tested at 10 km^2 intervals (Figure 3). The number of identified source patches declined as the threshold increased. When the threshold was below 100 km^2, the patch count decreased

sharply with each increment in the threshold. In contrast, once the threshold exceeded 100 km^2, the decline rate became more gradual. The 100 km^2 threshold represents a critical inflection point. Values below this level retain an excessive number of potentially fragmented small patches; however, thresholds above it yield diminishing marginal returns in enhancing the overall ecological functionality of the source patch set. Consequently, 100 km^2 was selected as the final threshold. This criterion aimed to identify core patches capable of sustaining stable internal species populations, ensuring the continuity of key ecological flows, and collectively forming an efficiently connected network at the regional scale. The identified sources possessed high ecosystem service and a highly interconnected structure. According to the patch connectivity index (dPC), the identified sources were assigned to high, medium, and low connectivity using the natural breaks method.

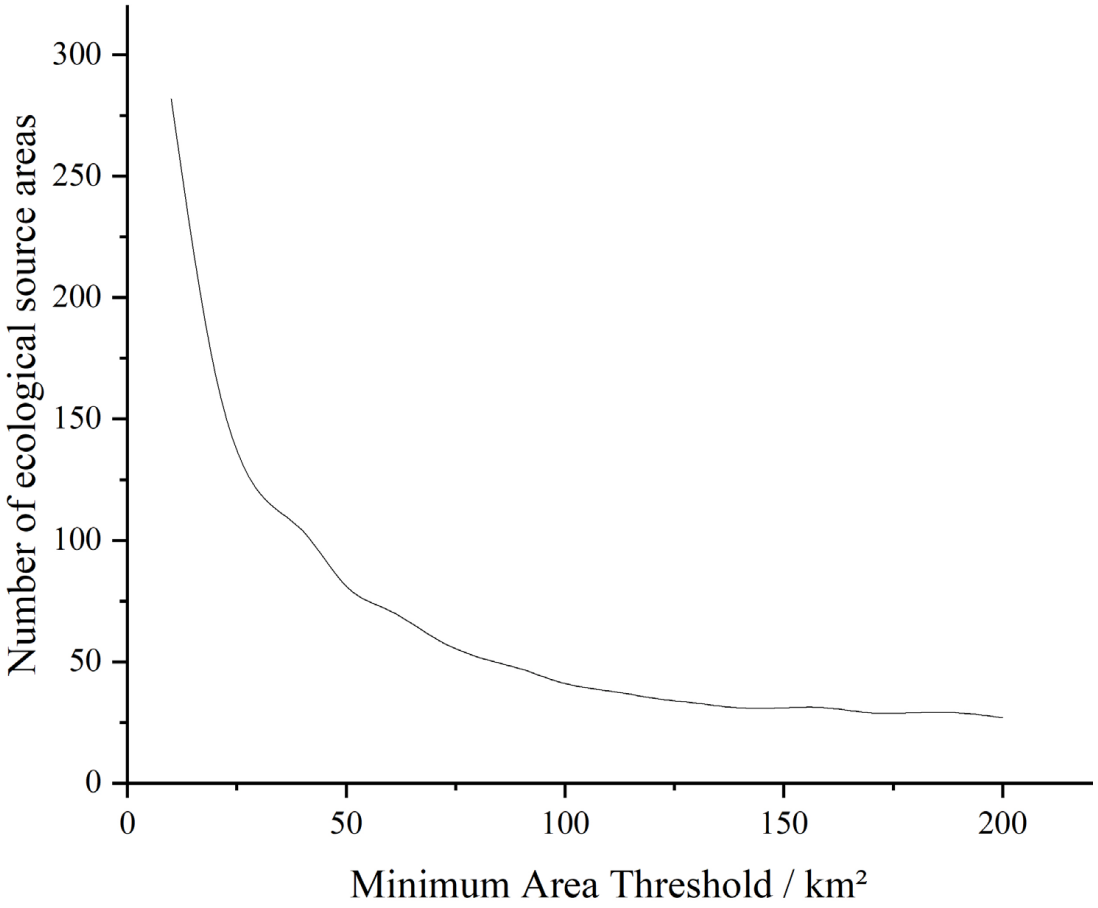

Figure 3. Variation in the setting of the ecological source area minimum area threshold.

(1) Quantification of ecosystem services

Based on the ecological background and unique regional characteristics of the BTH region, four ecosystem service functions were selected and quantified using corresponding methods. Habitat quality was quantified by coupling habitat suitability and disturbance levels, representing the biodiversity maintenance capacity of the ecosystem. This index is directly related to the preservation of regional biodiversity and serves as an important basis for assessing the health and carrying capacity of natural ecosystems [66]. Water conservation was quantified based on the balance between precipitation and evapotranspiration, reflecting the hydrological regulation function of the ecosystem. It played a critical role in water storage and runoff regulation in the BTH region, serving as a key support for ensuring regional water security and ecological balance [67,68]. Carbon sequestration was quantified by integrating aboveground and belowground biomass carbon, soil carbon, and

dead organic carbon pools, reflecting the climate regulation function of the ecosystem. Based on its significance in regulating regional climate, this service was incorporated into the research framework [69,70]. Soil conservation was quantified by coupling erosion factors and protective factors, representing the ecosystem's ability to maintain soil fertility and resist disturbances. Its level directly affected the sustainability of land productivity and served as an important foundation for the formation of regional ecological networks [71]. Table 1 presents the quantification methods for ecosystem services.

Table 1. Quantification of ecosystem services.

Ecosystem Service Function	Equation	Parameter Description
Habitat quality	$HQ_{ij} = H_{ij}[1 - \left(\frac{{D_{ij}}^z}{{D_{ij}}^z + K^z}\right)]$	HQ_{ij} represents the land use type's habitat quality j in grid i. $HQ_{ij} \in [0, 1]$, with a higher value indicating better habitat quality. H_{ij} denotes the habitat suitability. Half-saturation constant k is fixed at 0.5.
Water conservation	$WC_{ij} = \left[1 - \frac{AET_{ij}}{P_i}\right] \times P_i$	WC_{ij} denotes yearly water output at grid i, mm; P_i is cyclical precipitation; AET_{ij} represents the actual evapotranspiration at grid i.
Carbon sequestration	$CS_{tot} = CS_{above} + CS_{below} + CS_{soil} + CS_{dead}$	CS_{tot} represents entire carbon sequestration. CS_{above} as well as CS_{below} represent above-ground and below-ground biomass carbon sequestration, respectively; CS_{soil} represents the soil carbon sequestration; CS_{dead} represents dead organic matter carbon sequestration.
Soil conservation	$SC_i = R_i \cdot K_i \cdot LS_i \cdot (1 - C_i \cdot P_i) + R_i$	SC_i represents the soil conservation amount in grid i, t; R_i represents the sediment retention amount, t; K_i represents soil erodibility, t h MJ^{-1}mm^{-1}; LS_i represents slope distance and steepness factor (dimensionless); C_i and P_i represent vegetation-management and conservation practice factors, respectively.

(2) MSPA

Landscape ecology emphasized the coupling relationship between landscape structure and ecological processes. Grounded in the principles of mathematical morphology, MSPA utilized its theoretical framework to classify binary land use maps, identify patches critical to spatial form and connectivity, and analyze landscape morphology and spatial distribution characteristics [72]. Land cover types with ecological effects—specifically forest, grassland, and water zone—were assigned to the foreground, while the background comprised all other areas. Using MSPA in Guidos Toolbox 3.0 with an edge width of 150 m, the landscape comprised seven element types, e.g., core, bridge, islet, edge, perforation, branch, and loop [73]. This approach reflected the distinct roles played by various patches in the ecological flows. Core zones, representing larger habitat patches capable of providing ample habitat space and resources, were determined to be candidate ecological source areas [74].

2.4.2. Ecological Resistance Surface's Construction

The migration of ecological flows within landscapes was inevitably influenced by natural conditions and human disturbances. Achieving scientific rigor in path simulation necessitated the comprehensive quantification of multiple factors. The scientific selection

of resistance factors and the construction of an integrated resistance surface index system accurately characterized the degree of hindrance in the circulation process of regional ecological elements. A lower resistance value corresponded to a higher migration rate of ecological flow. Building on existing research [58,75,76], the work comprehensively considered the actual ecological characteristics and data availability in the BTH region. The selected resistance factors included land use type, elevation, slope, NDVI, ecosystem services, MSPA landscape types, and land use carbon emissions (Table 2).

Table 2. Ecological resistance factors.

Evaluation Factor	Grading Standard	Assignment	Weight	Evaluation Factor	Grading Standard	Assignment	Weight
Elevation (m)	−164~229	10	0.1069	MSPA	Core area	10	0.1908
	229~588	30			Bridge area and loop area	30	
	588~933	50			Branch and islet	50	
	933~1299	70			Edge as well as perforation	70	
	1299~2863	100			Background	100	
Slope (°)	0~5	10	0.1671	ES	0.63~1	10	0.0787
	5~14	30			0.52~0.63	30	
	14~23	50			0.33~0.52	50	
	23~33	70			0.10~0.33	70	
	33~76	100			0~0.10	100	
NDVI (normalized value)	0.79~1	10	0.1724	Carbon emission	−63.72~50	10	0.0779
	0.67~0.79	30			50~500	30	
	0.50~0.67	50			500~1000	50	
	0.07~0.50	70			1000~2000	70	
	0~0.07	100			2000~3207.40	100	
Land use type	Forest	1	0.2062	Land use type	Cropland	50	0.2062
	Water area	5			Unused land	70	
	Grassland	10			Construction land	100	

Reference was made to the empirical ranges commonly used in ecological corridor simulation to standardize measurement units and ensure comparability among the resistance factors. The resistance values for all factors were standardized within the range of 1–100. Avoiding low setting values was crucial as insufficient differentiation between resistance levels impeded the accurate characterization of ecological heterogeneity in the BTH region. This limitation was most pronounced in complex transitional zones like urban-rural fringes and mountain-plain interfaces. It also avoided excessively high values, which overstated the obstructing effect of local resistance on ecological flows. This standardized range aligned with the complexity of the ecosystem structure in the BTH region and the actual scope of ecological flow migration, enabling effective capture of the gradient differences in ecological resistance within the region.

For land use types and MSPA landscape types, their resistance values were determined based on existing research. The natural breaks method was employed to classify other continuous factors (e.g., elevation, slope, NDVI, ecosystem services, and carbon emissions) into five levels and assign corresponding resistance values. This classification method determines optimal intervals based on the inherent distribution characteristics of data, ensuring high homogeneity within each level while maximizing differences between levels. Finally, the entropy weight method was applied to calculate the objective weights of each index. After consistency validation, all resistance layers were weighted and overlaid using the ArcGIS 10.8 raster calculator to construct an integrated ecological resistance surface for the BTH region. This resistance surface aimed to quantify the hindering effects of spatial heterogeneity in the landscape matrix on ecological flow, serving as the foundation for the subsequent identification of corridors and obstacles.

2.4.3. Ecological Corridors' Extraction

Ecological corridors served as critical linear pathways connecting fragmented habitat patches within a landscape, essential for maintaining ecological connectivity. Ecological corridors were identified using circuit theory. This theory emphasized the multi-path diffusion characteristics of ecological flow in heterogeneous landscapes, overcoming the limitations of traditional single optimal path approaches. At its core, the framework employed a circuit analogy by conceptualizing habitat patches as nodes, landscape resistance as resistors, and the flow of ecosystem matter and energy as electrical current. This approach simulated potential corridors by modeling current flow, identifying the single least-cost paths and representing the potential movement network. The ecological corridors were derived from Linkage Mapper's Build Network and Map Linkages, which integrated the habitat patches and the resistance surface. According to the relevant reference [77] and the study area's characteristics, a cumulative cost distance threshold was set at 200,000. Thus, key corridors were extracted, facilitating species movement and ecological flows.

2.5. Multi-Objective Optimization of the Ecological Network

The work proposed a 3D collaborative optimization framework of barrier removal, structural robustness, and carbon sink enhancement for the BTH ecological network. The framework was developed from the identification of ecological obstacle points, improvement of ecological network topology, and regulation of land use carbon offset patterns. The core objective of the multi-objective optimization was to reduce connectivity resistance by removing ecological barriers, enhance network robustness through topological structure optimization, and improve carbon sink functionality by regulating carbon offset patterns. These three elements worked synergistically to enhance the ecological network's structure and function. The technical pathways were separately supported by circuit theory, complex network theory, and carbon cycle theory, integrating theoretical logic and optimization practices. The findings offer a scientific foundation for advancing ecological conservation and sustainable development in the BTH region.

2.5.1. Ecological Barrier Points' Identification

Ecological barrier points referred to high-resistance areas impeding connectivity between ecological sources and affecting species migration and dispersal [78]. The logic for identifying barrier points was derived from an extended application of circuit theory. When the diffusion of ecological flow was simulated using circuit theory, regions with high resistance formed resistance bottlenecks, which directly reduced the efficiency of ecological flow transmission. These bottleneck regions were identified as ecological barrier points. These points were identified through Linkage Mapper's Barrier Mapper module. Detection radius ranged from 500 to 1500 m, with a step size of 500 m. High-resistance areas located through the moving window method were designated as barrier points [79]. Removing such barrier points enhanced overall landscape connectivity, providing potential optimization directions for regional ecological connectivity.

2.5.2. Ecological Network's Topological Characteristics

The optimization of ecological network topology is fundamentally supported by complex network theory. This theory abstracts the complex interrelationships within real-world systems into a node-edge topological structure. This approach can precisely identify critical nodes and vulnerable links by leveraging properties such as small-world and scale-free characteristics to quantify the connections between elements [80]. The results provide a scientific basis for structural optimization [81]. An undirected topological network was built with nodes representing ecological source centroids and edges representing

ecological corridors. Subsequently, Gephi 0.10.1 was employed to calculate four node-specific attributes: betweenness, closeness, degree, as well as eigenvector centrality and two network-wide structural indices (i.e., clustering coefficient and modularity class). This methodology provided a more effective means of identifying implicit ecological connections than traditional approaches.

Specifically, a degree referred to the number of edges directly connected to a node, reflecting the local connectivity scale of an ecological source as a habitat. Structural islands with weak connections were identified within the network. Betweenness centrality measured the frequency with which a node acted as an intermediary on the shortest paths between other nodes. It was used to identify key nodes located on the shortest paths of numerous ecological flows. These nodes were potential ecological bottlenecks controlling the transmission of materials and species. Closeness centrality referred to the average shortest path distance from a node to all other nodes, characterizing the average accessibility efficiency of the node to other parts of the ecological network. Global accessibility efficiency was presented, and areas with low values were key to enhancing the overall resilience of the network. Eigenvector centrality combined a node's degree with the importance of its neighboring nodes, measuring the node's structural influence within the global network. Nodes with high values were typically the core elements maintaining network stability. Among network structural indices, the clustering coefficient was the ratio of the actual number of connections among a node's neighbors to the maximum possible number of connections. The local network clustering degree and connection redundancy were measured, with low values indicating areas vulnerable to connectivity loss. Modularity used a modularity optimization algorithm dividing nodes into groups. Connections within groups were dense, while those between groups were relatively sparse.

Indicator weights were assigned via the entropy weight method after normalizing the four nodes. A composite node importance value was then derived by weighted summation. A higher composite importance value reflected the greater functional significance of a habitat patch for ecological connectivity, flow facilitation, and overall system stability. Finally, network connectivity and stability were enhanced by adding nodes and edges according to the topological analysis.

2.5.3. Ecological Network Optimization Using Carbon Offset Pattern

(1) Carbon sequestration

The InVEST model quantified carbon sequestration. Based on the densities of soil carbon, below-ground biomass carbon, above-ground biomass carbon, and dead organic matter carbon pools, the sequestration amount was estimated [82]. The calculation process followed the same methodology as described in the ecosystem service carbon sequestration module above.

(2) Carbon emissions from land use

Land use-related carbon emissions comprise direct and indirect components. Direct carbon emissions (E_{direct}) from grassland, forest, cropland, water areas, and unused land are estimated directly using carbon emission coefficients (Equation (1)). Indirect ones ($E_{indirect}$) in construction zones are derived according to crude oil, gasoline, kerosene, coke, fuel oil, coal, diesel, natural gas, liquefied petroleum gas, and electricity's consumption converted into standard coal equivalents. Equation (2) employs the carbon emission coefficient method.

Carbon emissions show a positive correlation with the nighttime light index within a given region. The total energy-related carbon emissions for the BTH region are downscaled to the pixel level based on nighttime light data [40] (Equation (3)). Carbon emission allocation based on nighttime light data has certain limitations. High-brightness areas are

prone to light saturation, which causes deviations in carbon emission estimates at the grid scale in such regions and affects the accuracy of the estimation. Nonetheless, this method remains ineffective for the spatial simulation of carbon emissions at the regional scale. Its allocation reveals the overall spatial pattern of carbon emissions in the BTH region, characterized by higher emissions in the center and lower emissions in the periphery. Thus, the macro-level spatial trends of ecological resistance are analyzed:

$$CA_x = \sum_{j=1}^{j} C_j = \sum S_j \times a_j \quad (1)$$

$$CB_x = \sum_{k=1}^{k} e_k \times \beta_k \times \gamma_k \quad (2)$$

$$C_r = \frac{DN_r}{DN_c} \times C_c \quad (3)$$

where CA_x represents the total carbon emissions of the xth city; C_j, S_j, and α_j represent the carbon emissions, area, as well as the kth land use type's carbon emission coefficient, respectively. CB_x, e_k, β_k, and γ_k represent construction land's carbon emissions in the xth city, kth energy's total energy consumption, standard coal conversion coefficient, as well as carbon emission coefficient, respectively; C_r and DN_r represent grid scale and the nighttime light index's carbon emissions, respectively; DN_c and C_c represent the nighttime light index and the total carbon emissions of the administrative district where the grid is located, respectively.

(3) Carbon offset rate

Carbon offset reflects the critical ecological function of forest vegetation in regional carbon cycling and in achieving the dual carbon goals. It measures carbon sequestered by forest vegetation through ecosystem processes such as photosynthesis against the total carbon emissions in the region. The calculation of the carbon offset rate is derived from the carbon sink-source balance in carbon cycle theory. The carbon offset rate is calculated using grid cells as the basic evaluation units to meet the needs of spatial quantitative analysis. For each grid cell, actual carbon sequestration is divided by the total carbon emissions within the same grid. A quantitative measure is yielded, reflecting the forest carbon sink to offset carbon emissions [57]:

$$CO_r = \frac{CS_{tot}}{C_r} \quad (4)$$

where CO_r, CS_{tot}, and C_r represent the carbon offset rate, carbon sequestration, and carbon emissions at the grid scale, respectively.

(4) Ecological network optimization using land use carbon offset

Building upon low carbon offset, the work concentrates on the surrounding areas. First, existing ecological source areas and regions with slopes exceeding 25° are excluded. Subsequently, high-capacity carbon sink lands, like forests and water areas, are prioritized for selection as ecological nodes. Finally, ecological corridors are constructed between these nodes and the original ecological sources using circuit theory. Connectivity facilitated by these corridors enhances the nodes' regulatory influence on low carbon offset areas, which maintains the regional carbon balance.

2.6. Ecological Network Before and After Optimization Evaluation

2.6.1. Evaluation Using Ecological Network Structural Indices

Network structural indices provide a multi-dimensional quantification of ecological connectivity. Network cycle index α measures the overall connectivity of the ecological network. Higher α indicates greater connectivity, facilitating more efficient flows of energy

and information within the network. Line-point ratio index β functions as a key metric to evaluate the network structure's complexity. Higher β denotes a more developed network with stronger inter-nodal linkages. Connectivity index γ directly reflects connectivity among all nodes in the network [83]:

$$\alpha = (L - V + 1)/(2V - 5) \quad (5)$$

$$\beta = L/V \quad (6)$$

$$\gamma = L/3(V - 2) \quad (7)$$

where L, V, and D represent the count of ecological corridors, ecological nodes, and ecological corridors' total length, respectively.

2.6.2. Ecological Network Robustness Evaluation

Robustness refers to an ecological network's ability to sustain connectivity after some nodes' destruction [84]. Based on a constructed adjacency matrix, Python 3.12 is utilized to simulate both random and targeted attacks on the undirected topological ecological network. Random attacks simulate stochastic natural disturbances via random node removal. Conversely, strategic attacks simulate the destruction of core ecological areas by sequentially removing nodes, which are ranked in order of importance:

$$R = \frac{C}{N' - N} \quad (8)$$

where N', N, and C represent the initial network size, the count of nodes removed, and the largest post-removal component's size, respectively.

2.6.3. Evaluation of Ecological Network Carbon Sink Capacity

A carbon sink generally refers to the absorption and storage of CO_2 by ecosystems such as forests, grasslands, shrubs, watersheds, and wetlands. Its capacity is quantified using land use-based carbon sink estimation methodologies:

$$C_a = \sum_{j=1}^{j} U_j V_j \quad (9)$$

where C_a represents the total carbon sink; j represents the land use type, U_j represents the area of j; V_j represents its corresponding carbon sink coefficient [85]. Table 3 lists carbon sink coefficients for different land use types.

Table 3. Carbon sink coefficients for different land use types.

Land Use Type		Carbon Sink Coefficient ($t \cdot hm^{-2} \cdot a^{-1}$)
Forest		0.870
Grassland	High coverage	0.138
	Medium coverage	0.046
	Low coverage	0.021
Shrubland		0.230
Watershed		0.671
Wetland		0.567

3. Results

3.1. Results of Ecological Network Identification

3.1.1. Ecological Sources' Identification According to Ecosystem Service Functions and MSPA

(1) Ecosystem service functions

The distribution of ecosystem service functions varies significantly among different cities in the BTH region (Figure 4). The overall habitat quality demonstrates a gradient characteristic of being higher in the north and lower in the south. High-value areas for water conservation and carbon sequestration are concentrated in the northern mountainous forest belt, while the soil conservation function is particularly prominent in the hilly and mountainous regions of western and northern Hebei. A comprehensive distribution map of ecosystem service importance has been generated by overlaying various ecosystem service functions (Figure 5).

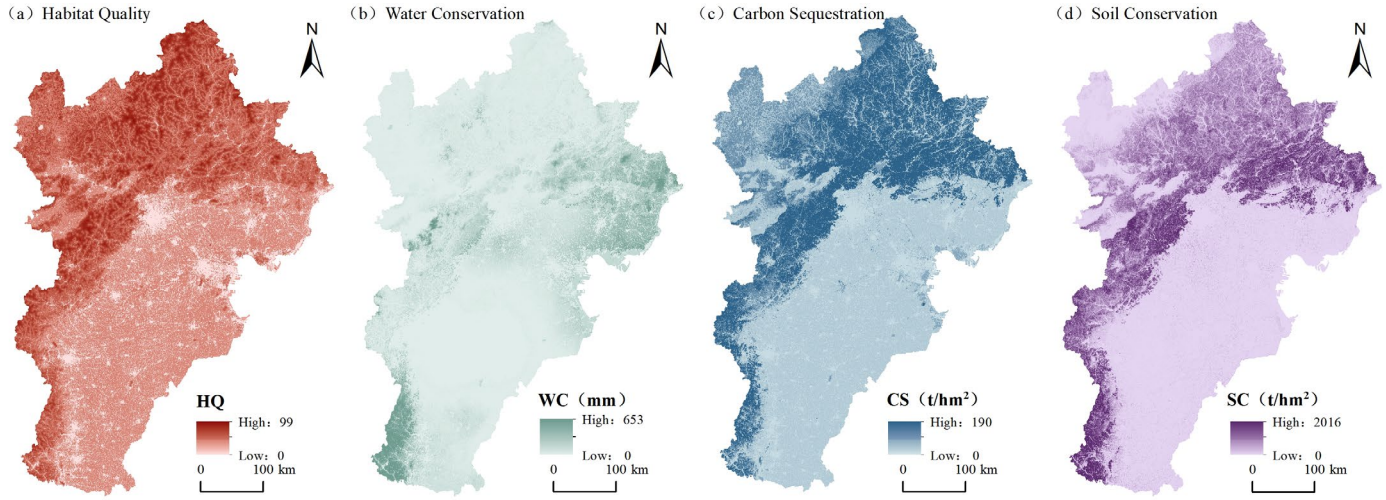

Figure 4. Ecosystem services' spatial distribution.

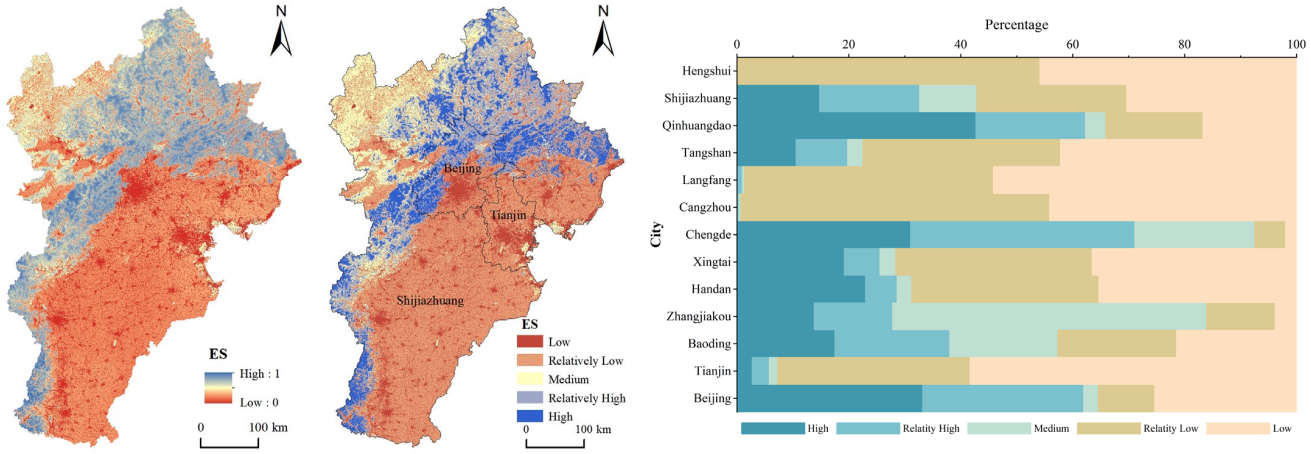

Figure 5. Distribution and percentage of comprehensive ecosystem service importance in the BTH region.

High-value zones account for 36.95% of Chengde, while relatively high-value zones make up 47.70%, indicating a prominent capacity for ecosystem service provision. Medium-value zones cover 57.47% of Zhangjiakou, with relatively high-value zones at 14.38% and high-value zones at 14.13%, reflecting good stability and continuity of ecosystem services. High-value zones account for 14.79% and relatively high-value zones for 12.81% in Beijing,

demonstrating that the city maintains a certain ecosystem service capacity despite rapid urbanization. In contrast, cities such as Cangzhou, Langfang, Hengshui, and Tianjin have very low proportions of high-value zones for ecosystem service importance, some even approaching zero. This may be related to accelerated urbanization, intensive human activities, and changes in land use types in these zones. Overall, the comprehensive importance of ecosystem services exhibits a northwest-high, southeast-low pattern.

(2) Morphological spatial pattern

MSPA using software Guidos Toolbox 3.0 identifies the distribution and area proportions of seven landscape types (Figure 6). The foreground area in the BTH region is 99,892.92 km^2, constituting approximately 46.17% total area. The core area constitutes the largest proportion, representing 51.95% foreground area. It is mainly distributed in the northern part of the region, with scattered distribution in the southwest and sparse distribution in the southeast.

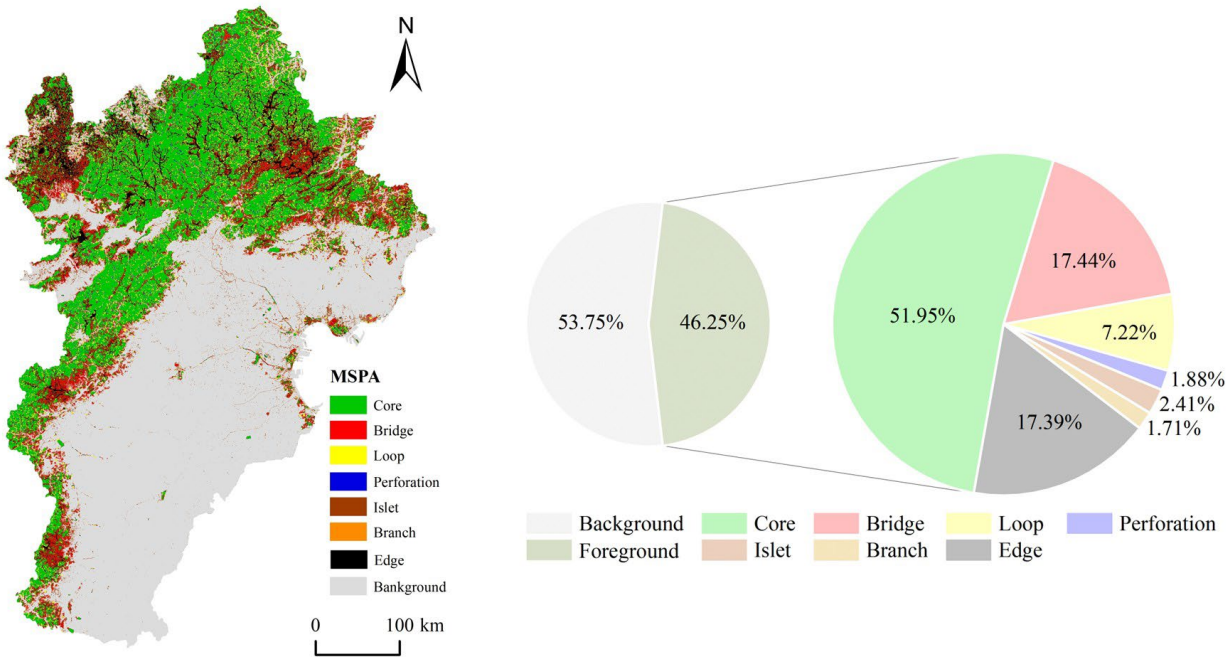

Figure 6. MSPA landscape types' spatial distribution as well as area proportions. Note: Pie charts on the left and right show each type's proportion relative to the entire study area and foreground area, respectively.

The bridge area covers 17,424.33 km^2 (accounting for 17.44% of the foreground area), indicating strong connectivity between core patches. The loop area, serving as a pathway for material and energy flow, occupies about 7.22% foreground area. The pore space, representing the core area's inner edge, accounts for a relatively small proportion. The significant internal habitat fragmentation necessitates improvements in connectivity and a stronger internal edge effect.

Islet patches are relatively small, covering about 2.41% of the foreground area. Located within the core area, they can potentially serve as stepping stones to provide habitats for biodiversity. Branches act as connecting pathways among the core, bridge, and loop areas. The edge area links the core areas with the background. It covers 17,369.62 km^2, accounting for 17.39% of the foreground area. Its unique location gives it distinct buffering characteristics. However, the southern part of the BTH region exhibits a relatively low landscape connectivity, with a lack of large and continuous habitat patches. It poses challenges to urban biodiversity conservation.

(3) Ecological sources identification

Based on ecosystem services and MSPA, a total of 41 ecological sources is determined (Figure 7), covering 25,426.27 km^2. The 31# ecological source is the largest (with an area of 5344.29 km^2), accounting for 21.02% overall zone. Area borders Chengde as well as Zhangjiakou. The second largest is the 12$^{\#}$ ecological source, situated at the border of Zhangjiakou, Beijing, and Baoding. It has an area of 3956.72 km^2, accounting for 15.56%. The primary land cover category is forest land, which significantly contributes to maintaining ecosystem health as well as stability.

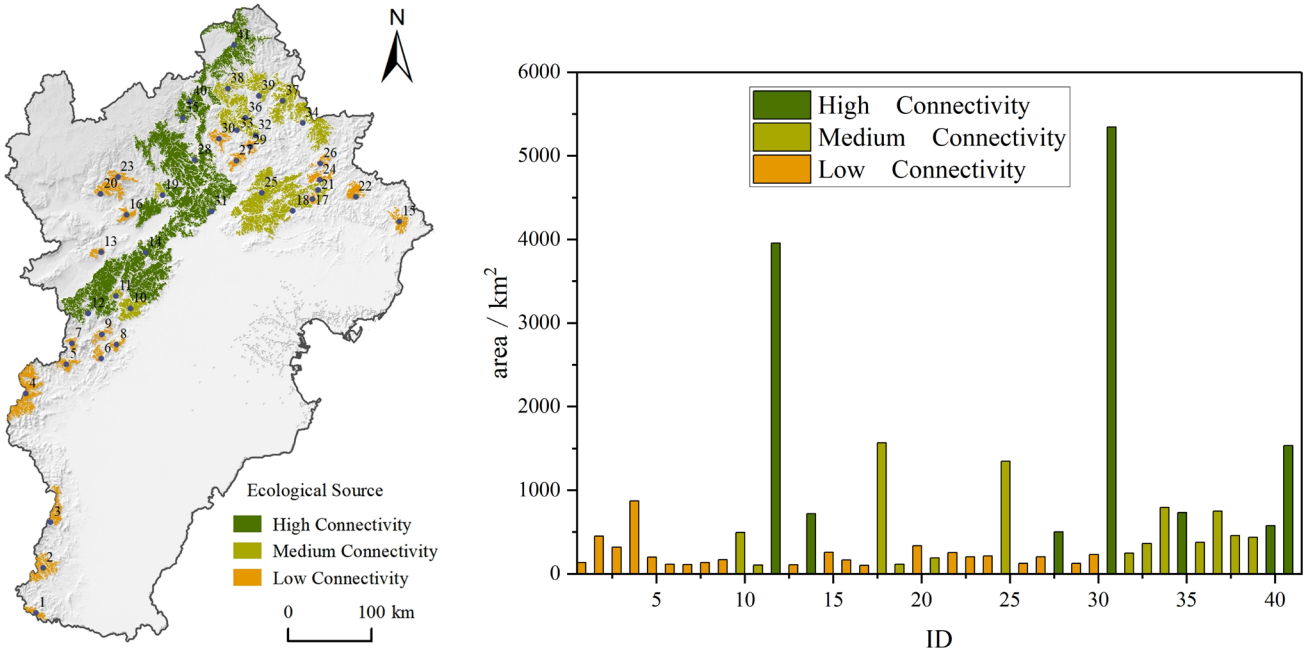

Figure 7. Spatial distribution of ecological sources and area statistics of source patches with different connectivity levels. Note: The numbers in the figure represent the ID of each ecological source.

3.1.2. Ecological Resistance Surface's Construction Using the MCR Model

Ecological resistance surface in the BTH region (Figure 8) reveals that low resistance values cluster in the northeastern and southwestern parts, such as Chengde and Qinhuangdao. These regions benefit from high vegetation coverage and abundant precipitation, which facilitate species migration and propagation. High resistance values correlate strongly with land use types associated with intensive human activity, particularly the urban construction land and transportation networks prevalent in Beijing, Tianjin, and other major Hebei cities' central urban areas. These areas significantly impede the movement of species and energy flow, demonstrating a clear link from ecological resistance's spatial distribution to the quality of natural conditions coupled with the intensity of anthropogenic interference.

3.1.3. Ecological Corridors' Extraction Based on Circuit Theory

The work identified 102 ecological corridors (Figure 9), extending 5886.36 km. These corridors, concentrated in the northern as well as southwestern sectors of the BTH region, formed a dense ecological connectivity pattern. In contrast, the southern and peripheral areas exhibit sparse nodes and weak connections, revealing significant gaps in ecological network coverage and structural weaknesses. This spatial distribution reflects a fragmented and poorly coordinated ecological landscape, which constrains the overall ecological functioning.

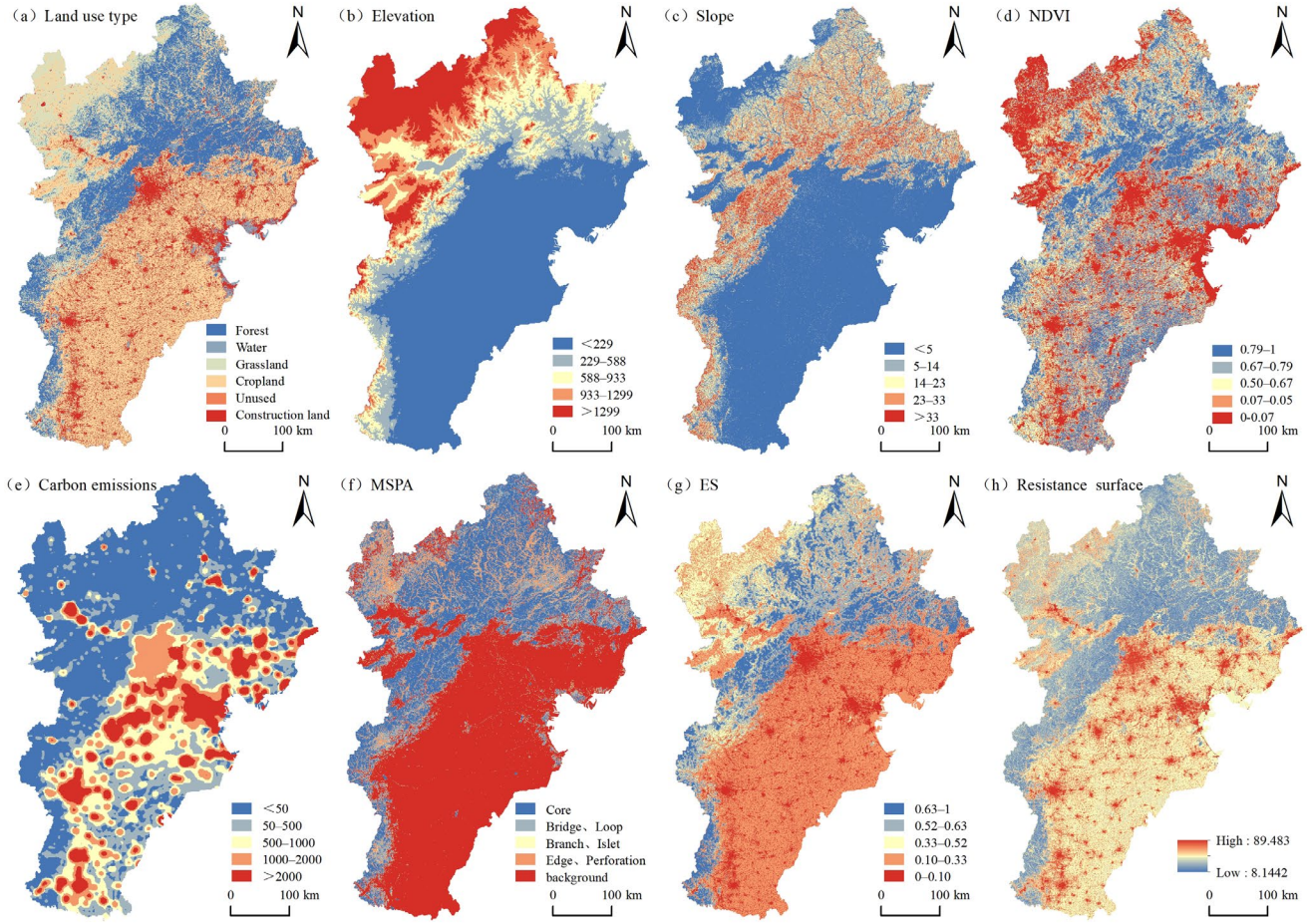

Figure 8. Spatial distribution of individual factor resistance surfaces and the comprehensive ecological resistance surface.

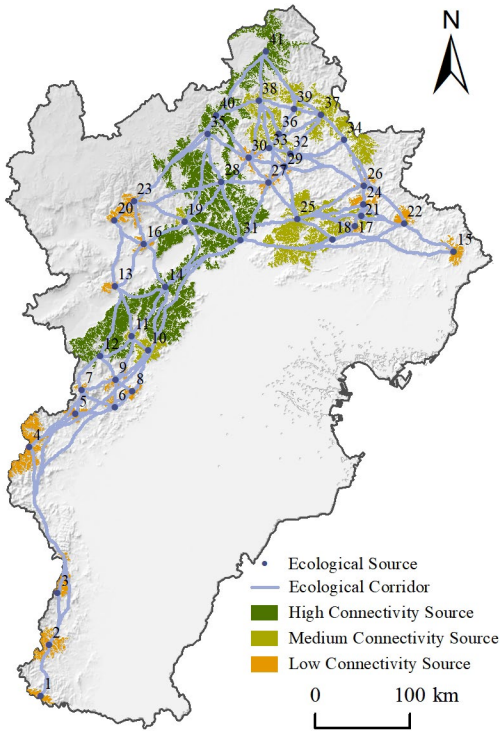

Figure 9. Ecological network's spatial distribution. Note: The numbers in the figure represent the ID of each ecological source.

3.2. Ecological Network's Multi-Dimensional Collaborative Optimization

3.2.1. Ecological Network Obstruction Points' Identification and Optimization

The ecological barrier points identified by Linkage Mapper exhibit a high spatial overlap with the corridors, directly impeding the transmission of ecological flows. Therefore, restoring barrier areas has been prioritized as the primary step in the optimization process. Utilizing ArcGIS 10.8 software, ecological barrier areas are assigned to five levels through the natural breaks method. Red areas represent elevated-value ecological barrier zones (Figure 10), covering an area of 565.56 km^2. Areas with high ecological barriers are distributed in concentrated patches, which significantly weaken the connectivity of ecological flow. Spatially, the barrier point density and barrier intensity are significantly higher in the northern mountainous areas of Chengde (Figure 10a,b), the northwestern mountainous regions of Baoding (Figure 10d,e), and southern Chengde (Figure 10f). Additionally, a localized high-barrier zone is observed in central Zhangjiakou (Figure 10c). Geomorphologically, the high-value barrier areas are primarily distributed in intermountain basins, extending along the Yan Mountain-Taihang Mountain range. This clustered distribution is strongly aligned with regional topographic gradients and land use intensity, reflecting how ecological processes are differentiated by natural geography and human activities.

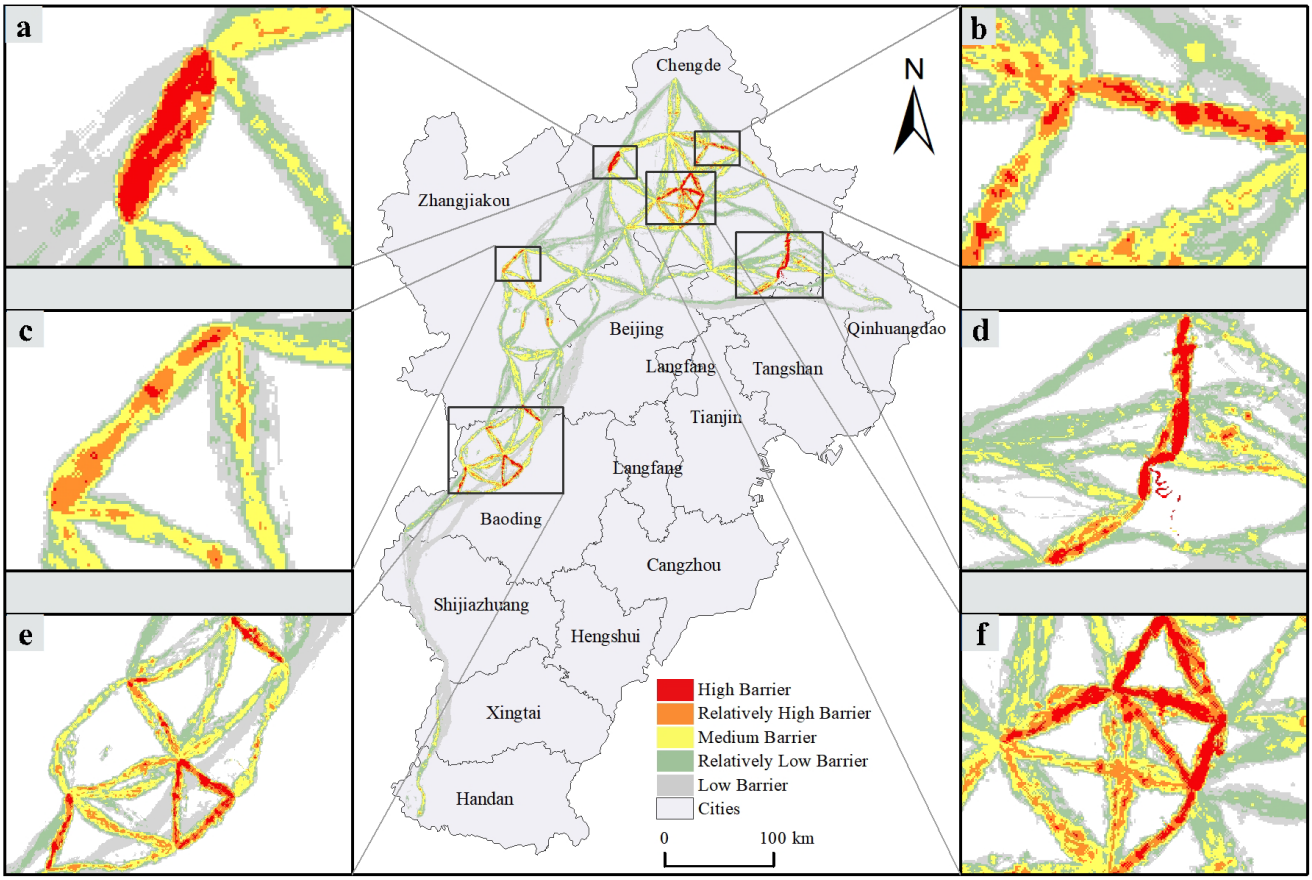

Figure 10. Spatial distribution of ecological barrier points.

When circuit theory is applied to connect ecological source areas, low-resistance paths are prioritized. However, there remain ecological corridors interrupted by high-resistance barrier points, highlighting an urgent need for restoration. Regional ecological connectivity will be enhanced by implementing native vegetation replanting in high-resistance areas within intermountain basins and establishing small ecological patches along mountainous barrier zones.

3.2.2. Ecological Network Optimization Using Complex Network Theory

(1) Ecological Network's Topological Structure

Abstract network comprises nodes (ecological sources) and edges (corridors) to construct an undirected topological network. The Gephi 0.10.1 platform is used to calculate topological metrics such as degree and betweenness centrality (Table 4) and generate a structural diagram of the ecological network (Figure 11). Node sizes correspond to their degrees. Node colors are differentiated by cool and warm tones to indicate degree values, with cool tones representing high-degree nodes and warm tones representing low-degree nodes. The cool-toned nodes centered around node 25 (e.g., nodes 22, 29, and 31) are larger in size and serve as key hubs in the network. They connect multiple ecological corridors and dominate the transmission of regional ecological flow. In contrast, the warm-toned peripheral nodes represented by nodes 1, 2, and 3 are smaller in size. They connect to fewer corridors, exhibiting lower efficiency in ecological flow transmission. The overall network exhibits a distinct structure characterized by core node dominance and inefficient peripheral connectivity. Clear targets are offered for subsequent topological optimization.

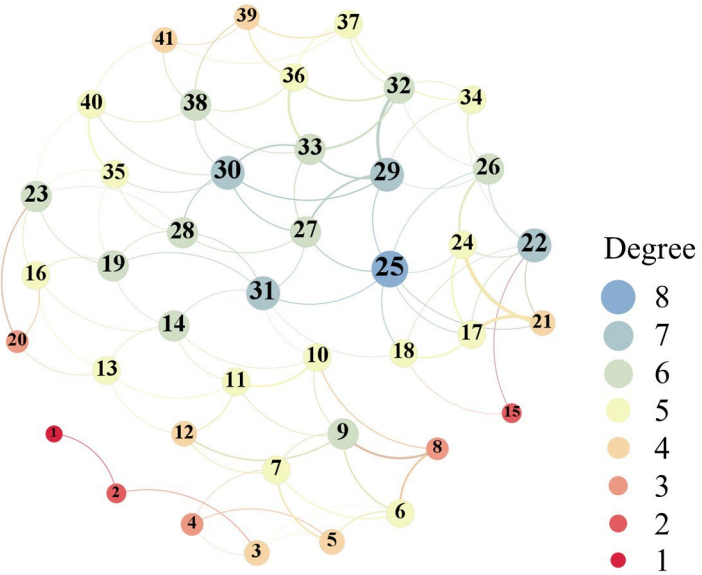

Figure 11. Topological structure of the BTH ecological network. Note: The numbers in the figure represent the ID of each ecological source.

Table 4. Topological metrics of the complex BTH network.

ID	D_i	B_i	C_i	E_i	CC_i	M_i	NCI_i	ID	D_i	B_i	C_i	E_i	CC_i	M_i	NCI_i
1	1	0.00	0.15	0.01	0.00	0	0.00	22	7	34.99	0.29	0.68	0.33	1	0.53
2	2	39.00	0.17	0.04	0.00	0	0.10	23	6	66.53	0.31	0.59	0.40	3	0.51
3	4	76.58	0.21	0.14	0.33	0	0.25	24	5	1.64	0.29	0.61	0.70	1	0.40
4	3	3.98	0.21	0.13	0.67	0	0.15	25	8	127.48	0.35	1.00	0.32	1	0.79
5	4	4.56	0.21	0.17	0.67	0	0.20	26	6	28.12	0.31	0.79	0.47	1	0.53
6	5	115.11	0.25	0.25	0.40	0	0.38	27	6	101.93	0.37	0.91	0.47	2	0.68
7	5	61.55	0.25	0.25	0.40	0	0.34	28	6	46.13	0.35	0.79	0.47	3	0.58
8	3	57.93	0.29	0.21	0.67	0	0.28	29	7	58.96	0.32	0.98	0.43	2	0.66
9	6	134.09	0.30	0.37	0.40	0	0.51	30	7	59.11	0.32	0.90	0.38	2	0.63
10	5	226.97	0.35	0.45	0.40	0	0.63	31	7	314.00	0.40	0.87	0.29	3	0.93

Table 4. *Cont.*

ID	D_i	B_i	C_i	E_i	CC_i	M_i	NCI_i	ID	D_i	B_i	C_i	E_i	CC_i	M_i	NCI_i
11	5	25.52	0.30	0.39	0.50	0	0.38	32	6	22.05	0.27	0.72	0.47	2	0.47
12	4	39.22	0.27	0.28	0.50	0	0.30	33	6	47.41	0.31	0.79	0.47	2	0.55
13	5	55.00	0.31	0.37	0.40	0	0.40	34	5	34.06	0.27	0.63	0.50	2	0.43
14	6	71.36	0.35	0.58	0.40	0	0.54	35	5	15.79	0.31	0.61	0.60	3	0.43
15	2	0.00	0.26	0.22	1.00	1	0.18	36	5	10.12	0.26	0.51	0.50	2	0.37
16	5	29.48	0.31	0.45	0.50	3	0.40	37	5	22.93	0.25	0.45	0.40	2	0.35
17	5	0.99	0.28	0.58	0.70	1	0.39	38	6	32.06	0.27	0.60	0.40	2	0.45
18	5	62.33	0.33	0.58	0.40	1	0.49	39	4	1.15	0.23	0.34	0.67	2	0.26
19	6	43.29	0.34	0.69	0.47	3	0.53	40	5	54.47	0.29	0.53	0.40	3	0.43
20	3	17.11	0.28	0.26	0.67	3	0.25	41	4	16.66	0.25	0.35	0.50	2	0.28
21	4	0.33	0.28	0.50	0.83	1	0.33								

Note: ID: Node ID; D_i: Degree; B_i: Betweenness Centrality; C_i: Closeness Centrality; E_i: Eigenvector Centrality; CC_i: Clustering Coefficient; M_i: Modularity Class; NCI_i: Node Comprehensive Importance.

Figure 12 shows the distribution of topological metrics for the BTH ecological network. The network has an average degree of 4.98, indicating a relatively simple overall structure. The majority of nodes (70.73%, 29 nodes) have a degree value of 5 or higher, suggesting stronger connectivity within northern as well as central zones. Twelve nodes (26.83%), all with degrees below 5, are primarily situated in the southern region and the northern periphery. These nodes form structural islets, which hinder regional ecological flow transmission.

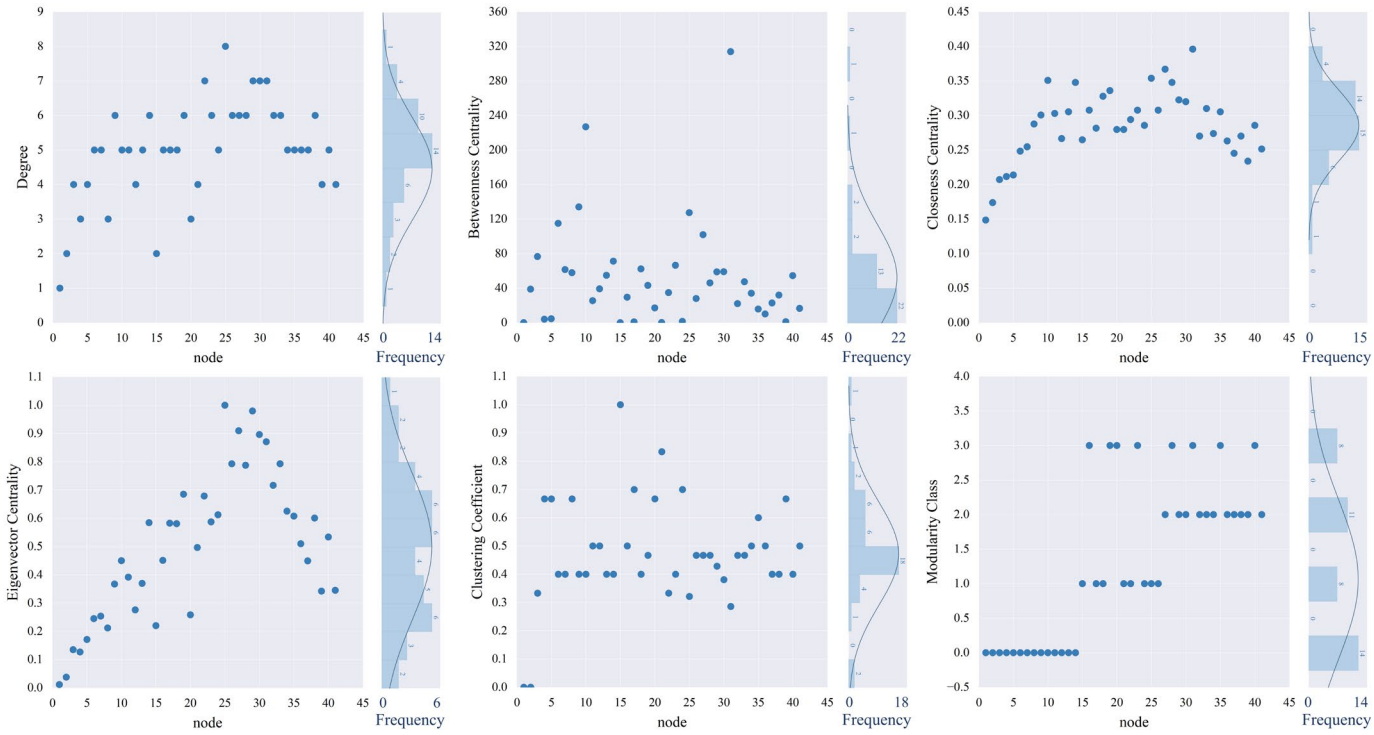

Figure 12. Distribution of topological indices in the BTH ecological network.

There is a significant disparity in node betweenness centrality. About 46.34% of the nodes (19 nodes) have a betweenness centrality > 40, among which 6 nodes have a

betweenness centrality > 100. These are primarily distributed along the Yan Mountains-Taihang Mountains range. While these areas serve as crucial habitats and migration pathways for species, their high centrality makes them prone to congestion due to overload. Simultaneously, nodes with low betweenness centrality, mostly located at the network edges, have limited capacity for ecological flow paths. The closeness centrality for the network generally falls between 0.15 and 0.40. Network resilience can be enhanced by activating peripheral nodes and diverting pressure away from the core nodes.

The ecological network's clustering coefficient varies between 0 and 1. The majority of nodes (34 nodes, 82.93%) exhibit high clustering coefficients above 0.4. About 16 nodes have coefficients of at least 0.5, demonstrating substantial clustering. However, several nodes with medium to low clustering coefficients exist in the study area's southern part, reflecting insufficient local connectivity. The modularity of the ecological network is 0.59, and the nodes are divided into 4 independent communities. Connections within the communities are tight, while connections between communities are relatively sparse.

The distribution of node comprehensive importance shows significant heterogeneity. High-value nodes such as nodes 31 and 25 constitute the core of maintaining ecosystem connectedness and robustness. Most nodes' importance values are concentrated between 0.2 and 0.6, maintaining basic ecological functions. Nodes 1, 2, and 15 are located on the network's periphery. Although their significance is relatively low, they still hold significance for local ecological functions. Ecological restoration measures (e.g., establishing stepping-stone zones along with short corridors) can enhance peripheral nodes' connectivity as well as the ecological network's overall stability.

(2) Optimization based on the ecological network's topological structure

Optimizing ecological networks based on topological structure is a core strategy for enhancing network stability. Building on the topological metrics calculated by Gephi 0.10.1, structural issues such as unbalanced node connectivity, congestion in core areas, and insufficient local connectivity have been identified. Accordingly, a multi-dimensional optimization strategy is developed by integrating degree, betweenness centrality, closeness centrality, and clustering coefficient (Figure 13).

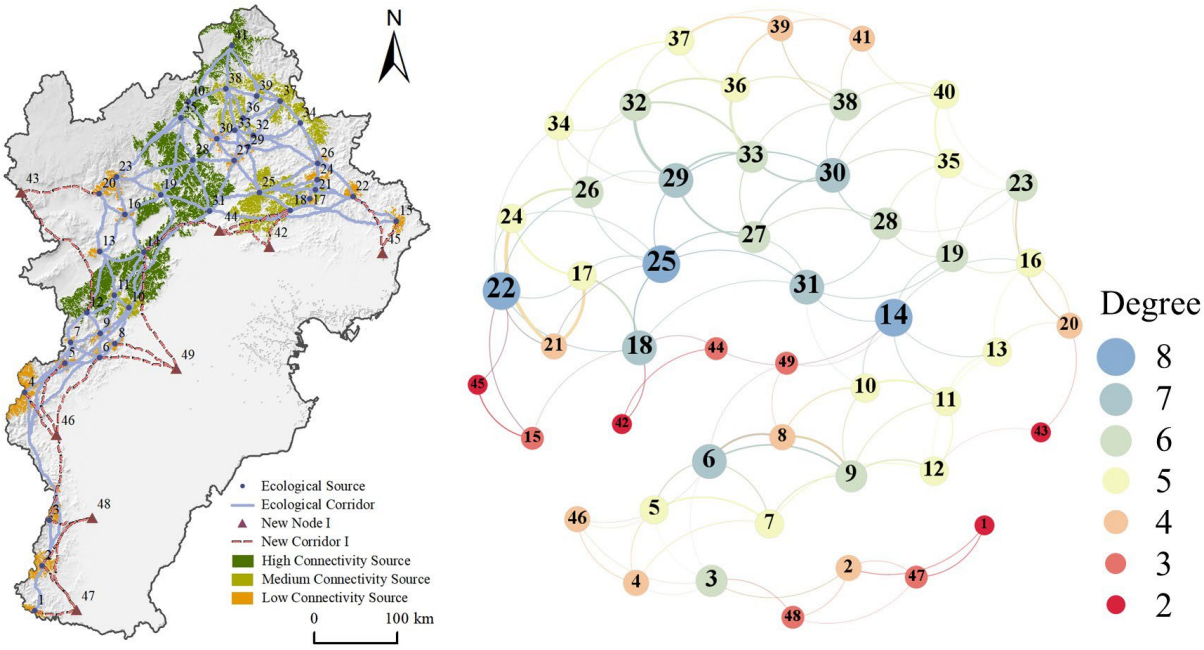

Figure 13. Optimized ecological network and structure using topology. Note: The numbers in the figure represent the ID of each ecological source.

Based on the complex network model, the identified low-connectivity nodes (with a degree ≤ 4) are distributed in the southern and northern peripheral regions, forming structural islets. Six auxiliary nodes (47, 45, 43, 46, 49, and 48) and 11 corridors are added after excluding inefficient nodes surrounded by larger patches to improve peripheral nodes' connectivity and network balance. Congested nodes with high betweenness centrality (over 100) are primarily distributed along the Yanshan-Taihang Mountains, where they are prone to bearing excessive ecological flow. Three bypass nodes (44, 49, and 42) and six corridors have been created to alleviate this bottleneck effect. Additionally, two nodes (47 and 45) and four corridors are supplemented. This intervention restricts ecological flow at certain nodes with zero betweenness centrality, which strengthens their connections to surrounding ecological units. The closeness centrality quantified by the model is below 0.25, indicating insufficient global accessibility efficiency. Therefore, stepping stones and nine corridors are added to enhance connectivity. Two auxiliary nodes (47 and 48) and four corridors are established to improve the local aggregation for low local clustering nodes with a clustering coefficient of 0.

A total of 8 new nodes and 20 ecological corridors are added by integrating the aforementioned optimization strategies and removing duplicate nodes and corridors, spanning 1981.83 km. They are primarily distributed around existing ecological corridors (Figure 13). The network's modularity increases to 0.61 after optimization. An improved community topology is beneficial for information transfer and material/energy exchange between communities.

3.2.3. Ecological Network Optimization Based on Land Use Carbon Offset

Using the InVEST model, spatial heterogeneity characterizes carbon sequestration across the BTH region (Figure 14a). High carbon sequestration areas cluster in Beijing's western mountains and northern Hebei, such as Zhangjiakou and Chengde. These areas are typified by ecological land uses (e.g., grasslands and forests), high vegetation coverage, and intact ecosystem structures. These characteristics provide a stable ecological foundation for carbon sequestration. Conversely, low carbon sequestration zones show a pronounced concentration in central and southern Hebei and the central urban area of Tianjin, particularly in cities such as Shijiazhuang, Handan, and Tangshan. These regions are classified as primary limited-carbon sequestration zones due to the high proportion of construction land and the severe fragmentation of ecological land.

Carbon emissions, along with carbon sequestration, exhibit distinct spatial complementarity (Figure 14b). High carbon emission areas are primarily concentrated in Tangshan, Handan, Shijiazhuang, and certain industrial zones in Tianjin. These regions are dominated by energy-intensive industries such as steel, chemicals, and building materials. They have high energy consumption intensity, serving as a regional carbon emission source. Low carbon emission areas tend to cluster in Zhangjiakou, Chengde, and Beijing's western mountainous regions. On one hand, these areas rely on low-carbon industrial systems like green energy and eco-tourism to reduce emissions. On the other hand, they synergize emission reduction and carbon sequestration due to their robust ecological foundation to enhance carbon sink capacity.

Based on carbon sequestration data calculated by the InVEST model and carbon emission data derived from nighttime light inversion, the carbon offset rate model is applied for quantification to derive the significant spatial heterogeneity of carbon offset capacity in the BTH region (Figure 14c). Low carbon offset values are concentrated in the urban cores (e.g., Tangshan, Tianjin) and surrounding industrial clusters, where economic activities hinder ecological flows. These areas are characterized by a weak ecological foundation and

high carbon emission pressures, highlighting the spatial imbalance between carbon sources and sinks.

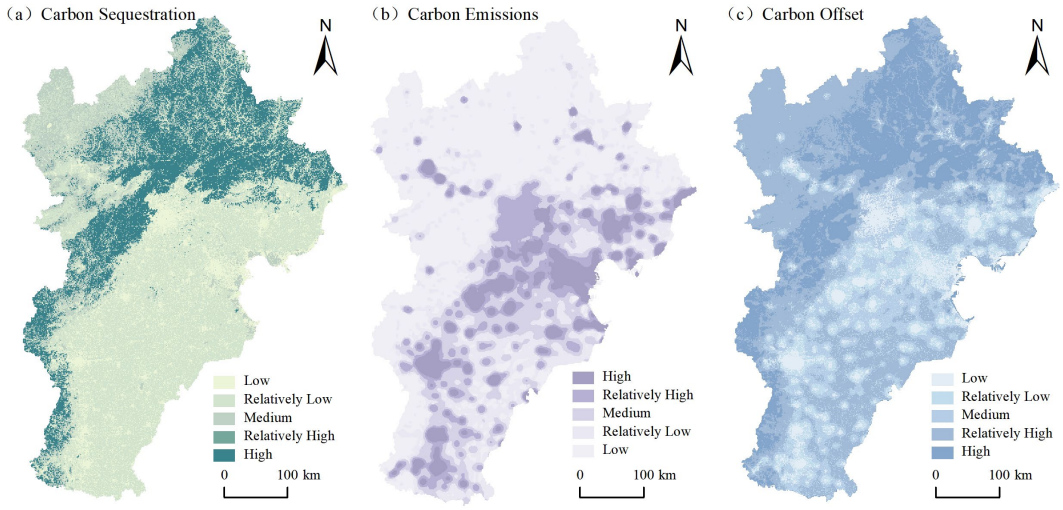

Figure 14. Spatial heterogeneity of carbon sequestration, carbon emissions, and carbon offset.

To optimize carbon offset efficiency and enhance ecological network connectivity, building upon prior topological structure optimization, large-area high-value carbon offset zones adjacent to low-value areas were selected as new ecological nodes (Figure 15). Priority was given to land types with outstanding carbon sequestration capacity, such as forested areas and water bodies. Additional stepping-stone nodes (50, 51, 52, and 53) were introduced to facilitate species dispersal, further strengthening the carbon compensation capacity of regional ecological sources and addressing gaps in ecological node identification in areas like Tangshan and Tianjin.

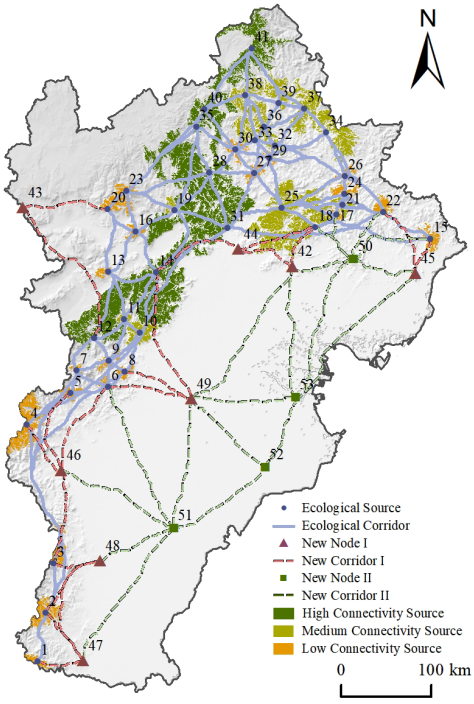

Figure 15. Ecological network optimized based on topology and carbon offset. Note: The numbers in the figure represent the ID of each ecological source.

A total of 19 new ecological corridors, spanning 2483.65 km, have been planned following circuit theory. They serve to connect the existing source points (nodes 1–41),

the topologically optimized new nodes (nodes 42–49), and the carbon offset-enhanced nodes (nodes 50–53) (Figure 15). These corridors primarily connect existing ecological networks and integrate with surrounding ecological security zones to achieve effective ecological connectivity. They focus on enhancing the connectivity of the ecological network in the southeastern Beijing-Tianjin-Hebei region, promoting the synergistic transmission of ecological flows and carbon sink functions.

The newly added ecological nodes and planned corridors should aim at enhancing ecological quality and environmental restoration, implemented through green infrastructure while avoiding disruption from economic activities. This strategy enhances the connectivity between carbon offset low value areas and ecological security zones, reduces ecological resistance, and achieves the coordinated promotion of economic development and ecological protection without affecting the development of key areas for economic growth.

3.3. Validation of Ecological Network Optimization Effects

3.3.1. Ecological Network Structural Indices

Ecological network's α, β, and γ increase by 12.99, 14.47, and 8.24%, respectively, after collaborative optimization of the topological structure and carbon offset capacity (Table 5). The optimized network demonstrates significant improvements in closure, corridor connectivity complexity, and overall connectivity. Connectivity density between ecological sources and path stability are enhanced to reduce the resistance to ecological flow transmission and strengthen the network's support capacity for key ecological processes.

Table 5. Ecological network structural indices before and after optimization.

Ecological Network Indices	Ecological Network Before Optimization	After Topology-Based Optimization	After Topology and Carbon Offset-Based Optimization
Network closure (α)	0.77	0.76	0.85
Network link-node ratio (β)	2.49	2.49	2.66
Network connectivity (γ)	0.87	0.87	0.92

3.3.2. Ecological Network Robustness

Robustness of the ecological network is assessed using random attacks and targeted attacks to simulate scenarios of natural disturbances and damage to core ecological areas, respectively. Targeted attacks cause significantly greater disruption to all three types of ecological networks (e.g., the pre-optimization network, the topology-optimized network, and the network with collaborative topology-carbon offset optimization) compared to random attacks. Additionally, the networks at different optimization stages exhibit distinct characteristics in their resistance to disturbances (Figure 16).

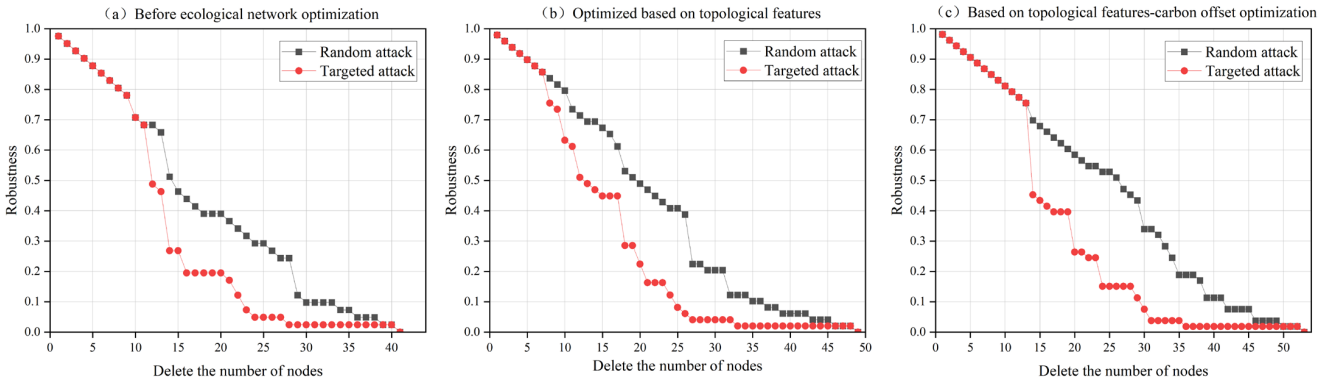

Figure 16. Changes in robustness of the ecological network.

The pre-optimization network demonstrates the lowest robustness, with its connectivity rate falling to 0.54 after 15 node removals and plummeting to 0.17 after 25. However, targeted removal of just 14 key nodes sharply declines to 0.32, revealing the network's vulnerability due to its over-reliance on a few core nodes.

The network optimized based on topological structure shows improved resistance to disturbances by adjusting connectivity between nodes. The connectivity rate is maintained at 0.63 after removing 15 nodes under random attacks. The connectivity rate drops to 0.31 only after removing 15 nodes during a targeted attack.

The collaboratively optimized topology-carbon offset network demonstrates the strongest resistance to disturbances. The connectivity rate remains at 0.53 even after the random removal of 20 nodes. The connectivity rate drops to 0.32 only after 18 critical nodes are removed under targeted attacks. Robustness stems from a multi-layered support structure formed by the newly added nodes and the core nodes, which distributes the risk of network failure. In summary, the disturbance resistance of the three network types demonstrates a gradient pattern. The collaboratively optimized network offers the strongest resistance, followed by the topological optimization and the original network. The optimization strategy of collaborative topology-carbon offset provides a more stable structural foundation for regional ecological security.

3.3.3. Ecological Network's Carbon Sink Capacity

According to the terrestrial carbon sink's estimation method, the carbon sink capacity of the BTH ecological network was evaluated before and after optimization. Overall carbon sink expanded from 2.0571 million tons before optimization to 2.1299 million tons after optimization, with a net increase of 72,800 tons. Patches contributed 68,400 tons to the increase, accounting for 93.99% total increase. As potent carbon-sink land types (mainly forests and water areas), the 12 newly added ecological nodes served to directly expand the scale of carbon sink carriers. Corridors contributed 4400 tons (6.01% of the total increase), mainly from protective forests along riverbanks and roadside vegetation. The increase in carbon sink from corridors was limited. The corridors also enhanced the vegetation growth vitality in adjacent original patches by connecting the material circulation channels of isolated patches, which indirectly promoted carbon sink growth. In general, the optimization measures enhanced the regional carbon sink capacity and alleviated ecological fragmentation around urban areas.

4. Discussion

4.1. Comparison with Existing Research

4.1.1. Identification of Sources Using Landscape Structure and Ecosystem Service Functions

Traditional methods for identifying ecological source areas rely on a single dominant driving factor. Using only landscape connectivity or ecosystem services as the core criterion overlooks the synergy between functionality and structure. The identified source areas may exhibit biases such as high functionality but weak connectivity or strong connectivity but low functionality [86,87]. A method integrating ecosystem services with MSPA is employed in this work to address this limitation. This approach eliminates fragmented patches with weak functionality and achieves a dual-dimensional screening based on structural connectivity and functional importance. The underlying rationale aligns with the work of Liang et al. [88] in the Qinghai-Tibet Plateau.

The work specifically targets the characteristics of the densely populated BTH region, where human disturbance is intense. The regional applicability of the theoretical framework has been enhanced by integrating multiple factors. The distribution of ecological source areas is relatively sparse in the southern part of the region, which closely aligns with the characteristics

of construction land encroaching on habitats and fragmented patch connectivity. This finding corroborates the conclusions of Liao et al. [89] regarding the compression of ecological space and insufficient habitat continuity in the area due to urbanization. Compared to traditional methods, this approach more accurately reflects the regional ecological stress conditions. It provides clear targets for subsequent ecological restoration and corridor construction in the southern area, preventing a disconnect between optimization measures and actual ecological problems.

4.1.2. Multi-Objective Optimization Pathways and Effectiveness Evaluation of the Ecological Network

A multi-objective optimization pathway of barrier removal, structural robustness, and carbon sink enhancement is constructed by integrating circuit theory, complex network theory, and carbon cycle theory. This framework addresses the limitation of existing studies, which prioritize connectivity as a single dimension [90]. Compared to traditional single-dimensional optimization approaches focusing on connectivity, the proposed multi-theoretical coupling framework can achieve multiple objectives, e.g., enhancing ecological flow and network disturbance resilience, as well as synergizing carbon sink functions. The theoretical construct resonates with Ref. [57] on karst regions; however, the work validates the enhanced carbon sequestration capacity. The proposed framework integrates carbon offset patterns to synergize structural and functional attributes. An optimization framework incorporating carbon offset patterns significantly enhances the ecological network's connectivity, stability, and carbon sink capacity. This success represents a key step towards synergistic structure-function optimization and provides a transferable paradigm for optimizing ecological networks in comparable regions. For areas with more complex terrain and higher urbanization levels, it is essential to strengthen the spatial representation of resistance factors with respect to microtopography, along with the adaptability of node and corridor layouts to built-up environments. This approach shall align with the characteristics of ecological flow transmission under more intense human disturbance.

A multi-dimensional evaluation framework is constructed to assess the optimization outcomes by integrating connectivity quantification, robustness simulation, and carbon sink accounting. This approach overcomes the limitations of previous studies that only verify connectivity [40] or stability [91]. Optimization is comprehensively examined through structural index analysis, disturbance simulation, and carbon sink evaluation. This multi-faceted approach is more systematic and scientific than traditional single-method evaluations, refining the evaluation system for ecological network optimization.

4.2. Practical Effectiveness of the Progressive Optimization Pathway for the Ecological Network

Network structure and carbon sink function are synergistically improved through topological optimization based on complex network theory and carbon offset optimization. Addressing structural deficiencies like node congestion and edge isolation through complex network theory significantly enhances the network's resistance to disturbance and its topological integrity. Robustness testing reveals that when 15 nodes are removed under random attack, the connectivity proportion increases from 0.54 to 0.63. When connectivity drops to a specific threshold, the number of nodes requiring removal in targeted attacks increases, indicating enhanced continuity in ecological flow transmission and improved structural resilience. With the beta and gamma indices stable and the alpha index decreasing by merely 0.01, the overall structural functionality remains largely unaffected.

The functional attributes of the network are enhanced by adding nodes in low-value carbon offset areas and constructing carbon synergy corridors after introducing the carbon cycle theory. The closure, line-point ratio, and connectivity increase by 12.99, 14.47, and 8.24%, respectively, after optimization, with robustness improved. The two optimization

pathways demonstrate strong compatibility and synergistic effects. Ultimately, the regional carbon sink increases by net 72,800 tons, with structural stability and enhanced carbon sequestration achieved.

From a theoretical perspective, structural optimization and functional optimization complement each other. The former establishes a stable carrier for ecological flows, while the latter enhances both connectivity and carbon sequestration capacity. Their synergy validates the proposed multi-objective optimization framework and broadens complex network theory's application in ecosystem and carbon cycle research. This provides a transferable technical paradigm to address the long-standing dilemma of ecological networks being structure-focused but function-neglected. The multi-objective optimization framework offers spatial decision-making support for regional ecological compensation and carbon sink regulation, facilitating the spatial implementation of the dual carbon policy.

4.3. Limitations and Future Research

Regarding the accuracy of carbon sink estimation, practical applicability, and the depth of theoretical integration, certain limitations exist. In terms of carbon sink estimation, the differential impact of ecological corridor width on carbon sequestration capacity and ecological flow transmission is not fully considered. It leads to potential estimation biases and a lack of specific guidance on optimal corridor width. For practical applicability, the work does not incorporate policy boundaries such as ecological protection red lines and basic farmland due to data constraints [56], which may affect the practicality of the proposed optimization scheme. In theoretical depth, although complex network theory and carbon cycle theory are combined, the analysis of their coupling mechanisms within ecological networks remains insufficient. The quantitative relationship between network structural characteristics and carbon sink function fails to be fully elucidated, which potentially limits the model's explanatory power in heterogeneous regions.

Future research should be directed toward several key areas for further development. First, carbon sink estimation models can be refined by incorporating corridor width gradients to enhance accuracy. Second, integrating spatial policy constraints will improve the practical feasibility of the proposed plans. Third, developing coupled structure-function models should be prioritized to elucidate the nonlinear relationships between key topological indicators and carbon sequestration capacity. This is critical for strengthening the mechanistic foundation of optimization pathways.

5. Conclusions

Taking the BTH region as the case study, the work developed an integrated framework of pattern recognition, structural optimization, functional synergy, and effectiveness evaluation. The framework systematically revealed the mechanisms for achieving enhanced ecological connectivity, increased network robustness, and synergistic gains in carbon sink function. Key findings were as follows.

5.1. Ecological Network's Spatial Configuration

The work delineated 41 ecological sources and 102 corridors, revealing a northwest-high, southeast-low density pattern. This disparity arose from the interplay of natural conditions and anthropogenic pressures. The pronounced gap in the southern ecological network indicated a spatial imbalance between conservation and development, calling for urgent interventions like ecological supplementation and enhanced connectivity.

5.2. Multi-Dimensional Problem Diagnosis and Optimization Pathways

A multi-objective optimization strategy titled barrier dredging, structural resilience, and carbon sink enhancement has been developed, synergistically improving the ecological

network. The first component was the ecological barrier dredging strategy. This involved implementing native vegetation restoration in high-resistance areas of intermontane basins and establishing small ecological patches along mountainous barrier zones. As a result, 565.56 km^2 of high-resistance ecological barriers have been eliminated to directly reduce the resistance to ecological flow transmission. The second component was the structural resilience optimization strategy. Approximately 8 auxiliary nodes and 20 ecological corridors have been added to address structural weaknesses such as nodes with a degree ≤ 4 (low connectivity) and nodes with a betweenness centrality > 100 (congested points). These optimized topological relationships enhanced the network's robustness. The third component was the carbon sink enhancement strategy. High carbon sink land types, such as woodlands and water bodies, were selected in areas with low carbon offset values. Additionally, 4 stepping-stone nodes and 19 carbon-synergistic corridors were established to strengthen the synergistic transmission of carbon sink functionality and ecological connectivity. These three strategies were progressively implemented and organically integrated to address structural and functional shortcomings in the network. The approach validated the synergistic optimization logic of first removing barriers, then optimizing structure, and finally enhancing carbon sinks.

5.3. Optimization Outcomes and Implementation Pathways

Post-optimization, the network connectivity metrics showed significant improvement, with the connectivity index, network connectivity probability, and loop connectivity increasing by 14.47, 8.24, and 12.99%, respectively. The restoration of barrier points directly enhanced ecological connectivity. Topological optimization primarily contributed to the network structure's robustness. Furthermore, carbon cycle theory boosted the system's carbon sequestration capacity, connectivity, and disturbance resistance. Notably, integrating the carbon cycle theory significantly enhanced connectivity. Future ecological restoration shall follow a sequential pathway: first mitigating barriers, then reinforcing structurally weak areas, and finally optimizing low carbon offset zones for targeted and effective governance.

5.4. Theoretical Innovations and Policy Implications

In summary, the multi-dimensional synergistic optimization framework developed in the work achieved the concurrent enhancement of both ecological network structure and carbon sink function. Theoretically, the work contributed to a paradigm shift in ecological network studies from structural optimization to functional synergy. A new paradigm was proposed, integrating structural robustness with carbon sink functionality. This provided a new theoretical perspective for coordinating the two global goals of biodiversity conservation and climate change mitigation. Methodologically, a systematic pathway was established, encompassing barrier identification, structural optimization, and carbon sink regulation.

This approach integrates circuit theory, complex network theory, and carbon cycle models for an interdisciplinary coupling of pattern, process, and function. The integrated multi-model technical pathway practiced herein holds reference value for developing universal spatial optimization methodologies. Practically, the findings provide a transferable decision-making reference for reconstructing BTH's ecological security pattern, synergistically advancing dual carbon goals, and informing national ecological spatial governance. The optimization logic and practical solutions developed for areas under intensive human disturbance can also serve as a case reference for sustainable spatial planning in other rapidly urbanizing or ecologically fragile regions worldwide.

Author Contributions: Conceptualization, Y.P., Z.Z., X.G. and P.Z.; Methodology, Y.P., X.G. and P.Z.; Software, Y.P. and Z.Z.; Validation, Y.P., Z.Z. and X.G.; Formal analysis, Y.P., Z.Z. and P.Z.; Investigation, Y.P.; Resources, Y.P., Z.Z., X.G. and P.Z.; Data curation, Y.P. and P.Z.; Writing—original draft, Y.P.; Writing—review & editing, Y.P., Z.Z., X.G. and P.Z.; Visualization, Y.P.; Supervision, Z.Z.,

X.G. and P.Z.; Project administration, Z.Z.; Funding acquisition, X.G. All authors have read and agreed to the published version of the manuscript.

Funding: This study was supported by the National Social Science Fund of China (Grant No. 25BGL241).

Data Availability Statement: The original contributions presented in the study are included in the article. Further inquiries can be directed to the corresponding author.

Conflicts of Interest: The authors declare no conflict of interest.

Abbreviations

BTH, BTH Urban Agglomeration; MSPA, morphological spatial pattern analysis; INVEST, Integrated Valuation of Ecosystem Services and Trade-offs; MCR, Minimum Cumulative Resistance Model; ESI, Ecosystem Service Importance; NDVI, Normalized Difference Vegetation Index; CO, Carbon Offset Rate; dPC, dProbability of Connectivity.

References

1. Yi, C.; Xu, B.; Shi, X.; Li, R.; Chen, J. Exploring the Spatial Effects of Rapid Urbanization on Land Use Efficiency in China Under Low-Carbon Constraints. *Ecol. Indic.* **2025**, *174*, 113442. [CrossRef]
2. Wu, W.; Xu, L.; Zheng, H.; Zhang, X. How Much Carbon Storage Will the Ecological Space Leave in a Rapid Urbanization Area? Scenario Analysis from Beijing-Tianjin-Hebei Urban Agglomeration. *Resour. Conserv. Recycl.* **2023**, *189*, 106774. [CrossRef]
3. Zhang, Y.; Wu, Q.; Fath, B.D. Review of Spatial Analysis of Urban Carbon Metabolism. *Ecol. Model.* **2018**, *371*, 18–24. [CrossRef]
4. Li, W.; Zhang, S.; Lu, C. Exploration of China's Net CO_2 Emissions Evolutionary Pathways by 2060 in the Context of Carbon Neutrality. *Sci. Total Environ.* **2022**, *831*, 154909. [CrossRef]
5. Feng, X.; Lin, X.; Li, Y.; Yang, J.; Yu, E.; He, C.; Lei, K.; Gao, W. Impact of Urban Land Development on Carbon Emission Performance Based on a Multidimensional Framework. *Environ. Impact Assess. Rev.* **2024**, *105*, 107429. [CrossRef]
6. Geng, J.; Yu, K.; Sun, M.; Xie, Z.; Huang, R.; Wang, Y.; Zhao, Q.; Liu, J. Construction and Optimisation of Ecological Networks in High-Density Central Urban Areas: The Case of Fuzhou City, China. *Remote Sens.* **2023**, *15*, 5666. [CrossRef]
7. Ma, J.; Yu, Q.; Wang, H.; Yang, L.; Wang, R.; Fang, M. Construction and Optimization of Wetland Landscape Ecological Network in Dongying City, China. *Land* **2022**, *11*, 1226. [CrossRef]
8. Li, Y.; Wei, M.; Zhou, R.; Jin, H.; Chen, Y.; Hong, C.; Duan, W.; Li, Q. Identifying Priority Restoration Areas Based on Ecological Security Pattern: Implications for Ecological Restoration Planning. *Ecol. Indic.* **2025**, *174*, 113486. [CrossRef]
9. Guo, Z.; Zhu, C.; Fan, X.; Li, M.; Xu, N.; Yuan, Y.; Guan, Y.; Lyu, C.; Bai, Z. Analysis of Ecological Network Evolution in an Ecological Restoration Area with the MSPA-MCR Model: A Case Study from Ningwu County, China. *Ecol. Indic.* **2025**, *170*, 113067. [CrossRef]
10. Tang, L.; Kasimu, A.; Chen, J. Ecological Deficit Mitigation in the Tianshan North Slope: Network-Driven Spatial Strategies for Ecosystem Service Flows. *Ecol. Indic.* **2025**, *178*, 113921. [CrossRef]
11. Avon, C.; Berges, L. Prioritization of Habitat Patches for Landscape Connectivity Conservation Differs between Least-Cost and Resistance Distances. *Landsc. Ecol.* **2016**, *31*, 1551–1565. [CrossRef]
12. Gao, X.; Yuan, Z.; Liu, X.; Liu, F.; Kou, C. Achieving Urban Ecosystem Resilience: Static and Dynamic Attack Simulation and Cascading Failure Analysis of Urban Blue-Green Infrastructure Networks. *Ecol. Indic.* **2025**, *179*, 114205. [CrossRef]
13. Sun, D.; Wu, X.; Wen, H.; Ma, X.; Zhang, F.; Ji, Q.; Zhang, J. Ecological Security Pattern Based on XGBoost-MCR Model: A Case Study of the Three Gorges Reservoir Region. *J. Clean. Prod.* **2024**, *470*, 143252. [CrossRef]
14. Li, J.; Liang, L.; Chao, Y.; Wang, X.; Qiu, M.; Luo, P.; Zhu, Y. Construction of the Ecological Security Pattern of Mu Us Sandy Land on the Basis of the "Source—Resistance—Corridor" Theory. *Ecol. Indic.* **2025**, *171*, 113162. [CrossRef]
15. Feng, Y.; Ping, L.; Hongliang, W.; Jianglin, Y. Evaluation of the Impact of Climate Change on the Ecological Resistance and Ecological Corridors Based on Set Pair Analysis Theory. *Ecol. Indic.* **2024**, *163*, 112050. [CrossRef]
16. Wang, S.; Zhang, R.; Wang, J.; Li, Q.; Wang, R.; Li, Y.; Zhang, L. Identification and Optimization of Ecological Corridors in the Middle Reaches of the Yellow River Basin. *J. Clean. Prod.* **2025**, *512*, 145676. [CrossRef]
17. Ding, G.; Guo, J.; Yi, D.; Ou, M.; Yang, G. Evaluating Habitat Isolation Driven by Future Urban Growth: A Landscape Connectivity Perspective. *Environ. Impact Assess. Rev.* **2025**, *113*, 107886. [CrossRef]
18. Tang, Y.; Gao, C.; Wu, X. Urban Ecological Corridor Network Construction: An Integration of the Least Cost Path Model and the InVEST Model. *ISPRS Int. J. Geo-Inf.* **2020**, *9*, 33. [CrossRef]

19. Tong, A.; Zhou, Y.; Chen, T.; Qu, Z. Constructing an Ecological Spatial Network Optimization Framework from the Pattern–Process–Function Perspective: A Case Study in Wuhan. *Remote Sens.* **2025**, *17*, 2548. [CrossRef]
20. Xiang, Q.; Yu, H.; Huang, H.; Li, F.; Ju, L.; Hu, W.; Yu, P.; Deng, Z.; Chen, Y. Assessing the Resilience of Complex Ecological Spatial Networks Using a Cascading Failure Model. *J. Clean. Prod.* **2024**, *434*, 140014. [CrossRef]
21. Nawaz, T.; Ansari, M.G.I.; Avirmed, B.; Zhao, T.; Liu, W.; Lian, J.; Wang, Y.; Liu, Y.; Zhao, J.; Yang, X.; et al. Ecological Network Optimization and Its Correlation with Net Primary Productivity in the Thal Desert: A 20-Year Analysis. *Geo-Spat. Inf. Sci.* **2025**, 1–25. [CrossRef]
22. Zhao, H.; He, J.; Liu, D.; Han, Y.; Zhou, Z.; Niu, J. Incorporating Ecological Connectivity into Ecological Functional Zoning: A Case Study in the Middle Reaches of Yangtze River Urban Agglomeration. *Ecol. Inform.* **2023**, *75*, 102098. [CrossRef]
23. Zhang, L.; Qiang, Z.; Xu, E. Improving the Ecological Network Optimization with Landscape Connectivity: A Case Study of Neijiang City, Sichuan Province. *Environ. Sci. Pollut. Res.* **2023**, *30*, 54753–54769. [CrossRef] [PubMed]
24. Gao, X.; Liang, X.; Guo, Z.; Yuan, Z.; Li, G.; Likulunga, L.E. The Analysis of Ecological Network Characteristics of Baiyangdian Basin in China Using the Complex Network Theory. *Ecol. Indic.* **2024**, *167*, 112650. [CrossRef]
25. Wu, Z.; Cheng, S.; Xu, K.; Qian, Y. Ecological Network Resilience Evaluation and Ecological Strategic Space Identification Based on Complex Network Theory: A Case Study of Nanjing City. *Ecol. Indic.* **2024**, *158*, 111604. [CrossRef]
26. Qin, J.; Dai, J.; Li, S.; Zhang, J.; Peng, J. Construction of Ecological Network in Qujing City Based on MSPA and MCR Models. *Sci. Rep.* **2024**, *14*, 9800. [CrossRef]
27. Yang, C.; Guo, H.; Huang, X.; Wang, Y.; Li, X.; Cui, X. Ecological Network Construction of a National Park Based on MSPA and MCR Models: An Example of the Proposed National Parks of "Ailaoshan-Wuliangshan" in China. *Land* **2022**, *11*, 1913. [CrossRef]
28. Na, Y.; Hong, Z.; Ren, S.; Huang, K. Optimizing the Construction of Ecological Networks in Beijing Using a Morphological Spatial Pattern Analysis—Minimal Cumulative Resistance Model. *Front. Environ. Sci.* **2024**, *12*, 1325880. [CrossRef]
29. Zhang, D.; Ren, H.; Sun, P.; Jing, P.; Guo, B. Construction of Multi-Level Ecological Security Network in Fragmented Nature Landscape Using the Three-Dimensional Framework of Ecological Adaptability. *Ecol. Indic.* **2023**, *157*, 111229. [CrossRef]
30. Liu, H.; Wang, Z.; Zhang, L.; Tang, F.; Wang, G.; Li, M. Construction of an Ecological Security Network in the Fenhe River Basin and Its Temporal and Spatial Evolution Characteristics. *J. Clean. Prod.* **2023**, *417*, 137961. [CrossRef]
31. Di Mauro, L.S.; Pluchino, A.; Conti, E.; Mulder, C. Ecological Validation of Soil Food-Web Robustness for Managed Grasslands. *Ecol. Indic.* **2022**, *141*, 109079. [CrossRef]
32. Bombrun, M.; Dash, J.P.; Pont, D.; Watt, M.S.; Pearse, G.D.; Dungey, H.S. Forest-Scale Phenotyping: Productivity Characterisation Through Machine Learning. *Front. Plant Sci.* **2020**, *11*, 99. [CrossRef] [PubMed]
33. Wang, T.; Huang, Y.; Cheng, J.; Xiong, H.; Ying, Y.; Feng, Y.; Wang, J. Construction and Optimization of Watershed-Scale Ecological Network Based on Complex Network Method: A Case Study of Erhai Lake Basin in China. *Ecol. Indic.* **2024**, *160*, 111794. [CrossRef]
34. Zhang, B.; Xie, Z.; Gao, J. Assessment on the Carbon Fixation of Urban Forests and Their Efficacy on Offsetting Energy Carbon Emissions in Shanghai. *Acta Ecol. Sin.* **2021**, *41*, 8906–8920. [CrossRef]
35. Wang, N.; Chen, X.; Zhang, Y.; Pang, J.; Long, Z.; Chen, Y.; Zhang, Z. Integrated Effects of Land Use and Land Cover Change on Carbon Metabolism: Based on Ecological Network Analysis. *Environ. Impact Assess. Rev.* **2024**, *104*, 107320. [CrossRef]
36. Zhao, Y.; Zhang, M.; Zhao, D.; Duo, L.; Lu, C. Optimizing the Ecological Network of Resource-Based Cities to Enhance the Resilience of Regional Ecological Networks. *Environ. Sci. Pollut. Res.* **2024**, *31*, 17156–17163. [CrossRef]
37. Qiu, S.; Yu, Q.; Niu, T.; Fang, M.; Guo, H.; Liu, H.; Li, S.; Zhang, J. Restoration and Renewal of Ecological Spatial Network in Mining Cities for the Purpose of Enhancing Carbon Sinks: The Case of Xuzhou, China. *Ecol. Indic.* **2022**, *143*, 109313. [CrossRef]
38. Wang, Z.; Xiao, L.; Yan, H.; Qi, Y.; Jiang, Q. Optimization of the Ecological Network Structure Based on Scenario Simulation and Trade-Offs/Synergies among Ecosystem Services in Nanping. *Remote Sens.* **2022**, *14*, 5245. [CrossRef]
39. Zhang, R.; Li, H.; Liu, Z. Synergistic Enhancement of Carbon Sinks and Connectivity: Restoration and Renewal of Ecological Networks in Nanjing, China. *Land* **2025**, *14*, 93. [CrossRef]
40. Lu, Z.; Geng, Y.; Li, W.; Yue, R. Integrating Spatial Carbon Factors into Ecological Network Construction in an Energy-Intensive Megaregion Toward Multi-Objective Synergy in Northern China. *Environ. Impact Assess. Rev.* **2024**, *106*, 107480. [CrossRef]
41. Song, S.; Gong, Y.; Yu, Y. Integrating Pattern, Process, and Function in Urban Landscape Ecological Network Planning: A Case Study of Harbin Central City. *Ecol. Indic.* **2024**, *159*, 111671. [CrossRef]
42. Zhang, W.; Fan, Y.; Wang, B. Ecological Network Construction Based on Ecosystem Services and Landscape Pattern Indices in the Tabu River Basin. *Land* **2024**, *13*, 2209. [CrossRef]
43. Vagge, I.; Chiaffarelli, G.; Pirola, L.; Gibelli, M.G.; Sgalippa, N.; Vagge, I.; Chiaffarelli, G.; Pirola, L.; Gibelli, M.G.; Sgalippa, N. Landscape Ecology and Ecosystem Services as Landscape Analysis and Assessment Tools for Ecological Landscape Planning. In *Landscape Architecture and Design—Sustainability and Management*; IntechOpen: London, UK, 2024.
44. Shen, J.; Zhu, W.; Peng, Z.; Wang, Y. Improving Landscape Ecological Network Connectivity in Urbanizing Areas from Dual Dimensions of Structure and Function. *Ecol. Model.* **2023**, *482*, 110380. [CrossRef]

45. Wang, X.; Wen, D.; Liu, P.; Wei, C.; Zhao, P.; Xu, N. Maintaining Ecological Connectivity in Highly Urbanized Areas: Optimal Strategy, Key Patches and Protection Policy. *Ecol. Indic.* **2024**, *164*, 112152. [CrossRef]
46. Chen, H.; Yan, W.; Li, Z.; Wende, W.; Xiao, S. A Framework for Integrating Ecosystem Service Provision and Connectivity in Ecological Spatial Networks: A Case Study of the Shanghai Metropolitan Area. *Sustain. Cities Soc.* **2024**, *100*, 105018. [CrossRef]
47. Guan, Y.; Zhang, F.; Feng, Q.; Wei, Y.; Li, G.; Song, Z. Ecological Security Pattern Construction Based on Multi-Scenario Trade-Offs of Ecosystem Services: A Case Study of the Shiyang River Basin. *Land* **2025**, *14*, 2159. [CrossRef]
48. Wang, X.; Tang, X.; Shi, J.; Du, P. Construction and Optimization of Urban and Rural Ecological Security Patterns Based on Ecological Service Importance in a Semi-Arid Region: A Case Study of Lanzhou City. *Sustainability* **2024**, *16*, 6177. [CrossRef]
49. Pan, J.; Wang, Y.; Zhang, Z. Identification and Optimization of Ecological Network in Arid Inland River Basin Using MSPA and Spatial Syntax: A Case Study of Shule River Basin, NW China. *Land* **2023**, *12*, 292. [CrossRef]
50. Zhou, J.; Hou, Q.; Li, W. Spatial Resilience Assessment and Optimization of Small Watershed Based on Complex Network Theory. *Ecol. Indic.* **2022**, *145*, 109730. [CrossRef]
51. Wan, Y.; Wang, Y.; Gao, M.; Jin, L. An Empirical Assessment of Whether Urban Green Ecological Networks Have the Capacity to Store Higher Levels of Carbon. *Sci. Rep.* **2024**, *14*, 3132. [CrossRef]
52. Cao, C.; Luo, Y.; Xu, L.; Xi, Y.; Zhou, Y. Construction of Ecological Security Pattern Based on InVEST-Conefor-MCRM: A Case Study of Xinjiang, China. *Ecol. Indic.* **2024**, *159*, 111647. [CrossRef]
53. Chen, R.; Zhang, S.; Huang, X.; Li, X.; Peng, J. Ecological Network Construction Based on Red, Green and Blue Space: A Case Study of Dali City, China. *ISPRS Int. J. Geo-Inf.* **2024**, *13*, 279. [CrossRef]
54. Xu, A.; Hu, M.; Shi, J.; Bai, Q.; Li, X. Construction and Optimization of Ecological Network in Inland River Basin Based on Circuit Theory, Complex Network and Ecological Sensitivity: A Case Study of Gansu Section of Heihe River Basin. *Ecol. Model.* **2024**, *488*, 110578. [CrossRef]
55. Cao, W.; Jia, G.; Yang, Q.; Sun, H.; Wang, L.; Svenning, J.-C.; Wen, L. Construction of Ecological Network and Its Temporal and Spatial Evolution Characteristics: A Case Study of Ulanqab. *Ecol. Indic.* **2024**, *166*, 112344. [CrossRef]
56. Song, S.; Xu, D.; Hu, S.; Shi, M. Ecological Network Optimization in Urban Central District Based on Complex Network Theory: A Case Study with the Urban Central District of Harbin. *Int. J. Environ. Res. Public Health* **2021**, *18*, 1427. [CrossRef]
57. Huang, K.; Peng, L.; Wang, X.; Deng, W.; Liu, Y. Incorporating Circuit Theory, Complex Networks, and Carbon Offsets into the Multi-Objective Optimization of Ecological Networks: A Case Study on Karst Regions in China. *J. Clean. Prod.* **2023**, *383*, 135512. [CrossRef]
58. Men, D.; Pan, J. Ecological Network Identification and Connectivity Robustness Evaluation in the Yellow River Basin Under a Multi-Scenario Simulation. *Ecol. Model.* **2023**, *482*, 110384. [CrossRef]
59. Xu, C.; Chen, X.; Yu, Q.; Avirmed, B.; Zhao, J.; Liu, W.; Sun, W. Relationship Between Ecological Spatial Network and Vegetation Carbon Use Efficiency in the Yellow River Basin, China. *GIScience Remote Sens.* **2024**, *61*, 2318070. [CrossRef]
60. Yang, J.; Huang, X. The 30 m Annual Land Cover Datasets and Its Dynamics in China from 1985 to 2023. *Earth Syst. Sci. Data* **2024**, *13*, 3907–3925. [CrossRef]
61. Wu, Y.; Shi, K.; Chen, Z.; Liu, S.; Chang, Z. *An Improved Time-Series DMSP-OLS-Like Data (1992–2023) in China by Integrating DMSP-OLS and SNPP-VIIRS 2021*; Harvard Dataverse Dataset: Cambridge, MA, USA, 2021.
62. Guan, H.; Bai, Y.; Tang, Y.; Zhang, C.; Zou, J. Spatial Identification and Optimization of Ecological Network in Desert-Oasis Area of Yellow River Basin, China. *Ecol. Indic.* **2023**, *147*, 109999. [CrossRef]
63. Xue, J.; Li, Z.; Feng, Q.; Gui, J.; Zhang, B. Construction of Ecological Conservation Pattern Based on Ecosystem Services of Three River Headwaters, Western China. *Glob. Ecol. Conserv.* **2023**, *44*, e02491. [CrossRef]
64. Nie, H.; Zhao, Y.; Zhu, J.; Ning, A.; Zheng, W. Ecological Security Pattern Construction in Typical Oasis Area Based on Ant Colony Optimization: A Case Study in Yili River Valley, China. *Ecol. Indic.* **2024**, *169*, 112770. [CrossRef]
65. Huang, K.; Peng, L.; Wang, X.; Deng, W. Integrating Circuit Theory and Landscape Pattern Index to Identify and Optimize Ecological Networks: A Case Study of the Sichuan Basin, China. *Environ. Sci. Pollut. Res.* **2022**, *29*, 66874. [CrossRef] [PubMed]
66. Yuan, Q.; Li, R. Priority Conservation Zoning for Future Karst Areas Based on the Construction of a Multi-Perspective Ecological Security Pattern. *Ecol. Indic.* **2025**, *178*, 113941. [CrossRef]
67. Gupta, S.; Borrelli, P.; Panagos, P.; Alewell, C. An Advanced Global Soil Erodibility (K) Assessment Including the Effects of Saturated Hydraulic Conductivity. *Sci. Total Environ.* **2024**, *908*, 168249. [CrossRef]
68. Chen, Z.; Lin, J.; Huang, J. Linking Ecosystem Service Flow to Water-Related Ecological Security Pattern: A Methodological Approach Applied to a Coastal Province of China. *J. Environ. Manag.* **2023**, *345*, 118725. [CrossRef]
69. He, Y.; Xia, C.; Shao, Z.; Zhao, J. The Spatiotemporal Evolution and Prediction of Carbon Storage: A Case Study of Urban Agglomeration in China's Beijing-Tianjin-Hebei Region. *Land* **2022**, *11*, 858. [CrossRef]
70. Yu, Y.; Guo, B.; Wang, C.; Zang, W.; Huang, X.; Wu, Z.; Xu, M.; Zhou, K.; Li, J.; Yang, Y. Carbon Storage Simulation and Analysis in Beijing-Tianjin-Hebei Region Based on CA-Plus Model Under Dual-Carbon Background. *Geomat. Nat. Hazards Risk* **2023**, *14*, 2173661. [CrossRef]

71. Wu, S.; Zhao, C.; Yang, L.; Huang, D.; Wu, Y.; Xiao, P. Spatial and Temporal Evolution Analysis of Ecological Security Pattern in Hubei Province Based on Ecosystem Service Supply and Demand Analysis. *Ecol. Indic.* **2024**, *162*, 112051. [CrossRef]
72. Guo, J.; Feng, P.; Xue, H.; Xue, S.; Fan, L. A Framework of Ecological Security Patterns in Arid and Semi-Arid Regions Considering Differences Socioeconomic Scenarios in Ecological Risk: Case of Loess Plateau, China. *J. Environ. Manag.* **2025**, *373*, 123923. [CrossRef]
73. Chen, J.; Li, P.; Wang, H. MSPA-Based Collaborative Evaluation and Planning Governance of Territory and Natural Environment in Metropolitan Agglomerations—A Case Study of EGIDDZ in Yangtze River Delta. *J. Resour. Ecol.* **2024**, *15*, 1263–1273. [CrossRef]
74. Wang, Y.; Qu, Z.; Zhong, Q.; Zhang, Q.; Zhang, L.; Zhang, R.; Yi, Y.; Zhang, G.; Li, X.; Liu, J. Delimitation of Ecological Corridors in a Highly Urbanizing Region Based on Circuit Theory and MSPA. *Ecol. Indic.* **2022**, *142*, 109258. [CrossRef]
75. Men, D.; Pan, J. Incorporating Network Topology and Ecosystem Services into the Optimization of Ecological Network: A Case Study of the Yellow River Basin. *Sci. Total Environ.* **2024**, *912*, 169004. [CrossRef] [PubMed]
76. Xu, X.; Wang, S.; Rong, W. Construction of Ecological Network in Suzhou Based on the PLUS and MSPA Models. *Ecol. Indic.* **2023**, *154*, 110740. [CrossRef]
77. Kong, L.; Wang, Y.; Liu, Y.; Ao, Y.; Chai, B. Identification of Key Areas for Ecological Restoration Based on Ecological Carrying Capacity and Ecological Security Pattern: A Case Study of Baoding, the Central City of the Beijing-Tianjin-Hebei World-Class Urban Cluster. *Ecol. Indic.* **2025**, *178*, 114032. [CrossRef]
78. Yang, D.; Gao, Y.; Chen, J.; Li, X.; Li, Z.; Shen, L.; Yang, C. Optimizing Regional Ecological Security Patterns Based on Interpretable Machine Learning Models: A Case Study of Huzhou, Zhejiang Province. *J. Environ. Manag.* **2025**, *393*, 126905. [CrossRef]
79. McRae, B.H.; Hall, S.A.; Beier, P.; Theobald, D.M. Where to Restore Ecological Connectivity? Detecting Barriers and Quantifying Restoration Benefits. *PLoS ONE* **2012**, *7*, e52604. [CrossRef]
80. Li, T.; Li, M.; Liang, J.; Li, D.; Huang, X.; Liu, Q. Optimizing Ecological Networks for Rare and Endangered Plants: An Integration of Complex Network Analysis and Circuit Theory. *J. Environ. Manag.* **2025**, *393*, 127206. [CrossRef]
81. Xu, W.; Wang, J.; Zhang, M.; Li, S. Construction of Landscape Ecological Network Based on Landscape Ecological Risk Assessment in a Large-Scale Opencast Coal Mine Area. *J. Clean. Prod.* **2021**, *286*, 125523. [CrossRef]
82. Xu, G.; Xiong, K.; Shu, T.; Shi, Y.; Chen, L.; Zheng, L.; Fan, H.; Zhao, Z.; Yang, Z. Bundling Evaluating Changes in Ecosystem Service Under Karst Rocky Desertification Restoration: Projects a Case Study of Huajiang-Guanling, Guizhou Province, Southwest China. *Environ. Earth Sci.* **2022**, *81*, 302. [CrossRef]
83. Yang, H.; Xu, W.; Chen, Z.; Xie, X.; Yu, J.; Lei, X.; Guo, S.; Ding, Z. Ecological Network Construction for Bird Communities in High-Density Urban Areas: A Perspective of Integrated Approaches. *Ecol. Indic.* **2024**, *158*, 111592. [CrossRef]
84. Liu, M.; Peng, J.; Dong, J.; Jiang, H.; Xu, D.; Meersmans, J. Trade-Offs of Landscape Connectivity Between Regional and Interregional Ecological Security Patterns in a Junction Area of Beijing-Tianjin-Hebei Region. *Appl. Geogr.* **2024**, *167*, 103272. [CrossRef]
85. Guo, H.; Yu, Q.; Pei, Y.; Wang, G.; Yue, D. Optimization of Landscape Spatial Structure Aiming at Achieving Carbon Neutrality in Desert and Mining Areas. *J. Clean. Prod.* **2021**, *322*, 129156. [CrossRef]
86. Luo, J.; Zhu, L.; Fu, H. Construction of Wetland Ecological Network Based on MSPA-Conefor-MCR: A Case Study of Haikou City. *Ecol. Indic.* **2024**, *166*, 112329. [CrossRef]
87. Zhou, G.; Huan, Y.; Wang, L.; Lan, Y.; Liang, T.; Shi, B.; Zhang, Q. Linking Ecosystem Services and Circuit Theory to Identify Priority Conservation and Restoration Areas from an Ecological Network Perspective. *Sci. Total Environ.* **2023**, *873*, 162261. [CrossRef]
88. Liang, T.; Chen, Y.; Lu, X.; Zhou, Y.; Mao, Y.; Yang, F. Ecological Security Pattern Construction of the Qinghai-Tibet Plateau: A Comprehensive Evaluation Based on Multiple Sources and Resistance Surfaces. *Adv. Space Res.* **2025**, *76*, 4213–4234. [CrossRef]
89. Liao, M.; Zhang, Z.; Yan, R.; Bai, K. The Assessment of Biodiversity Changes and Sustainable Agricultural Development in the Beijing-Tianjin-Hebei Region of China. *Sustainability* **2024**, *16*, 5678. [CrossRef]
90. Liang, G.; Niu, H.; Li, Y. A Multi-Species Approach for Protected Areas Ecological Network Construction Based on Landscape Connectivity. *Glob. Ecol. Conserv.* **2023**, *46*, e02569. [CrossRef]
91. Wang, Y.; Zhang, F.; Chen, W.Y.; Meraj, G.; Kumar, P.; Chan, N.W.; Tan, M.L. Critical Phase Transitions and Early-Warning Frameworks for Ecological Networks in Typical Arid Regions. *J. Clean. Prod.* **2025**, *531*, 146888. [CrossRef]

Disclaimer/Publisher's Note: The statements, opinions and data contained in all publications are solely those of the individual author(s) and contributor(s) and not of MDPI and/or the editor(s). MDPI and/or the editor(s) disclaim responsibility for any injury to people or property resulting from any ideas, methods, instructions or products referred to in the content.